

**Transient Overvoltages Caused by a Monopolar Fault on a
Bipolar dc Overhead Line with Dedicated Metallic Return**

by

Raghu Ram Atmuri

A thesis submitted to the Faculty of Graduate Studies of
The University of Manitoba
in partial fulfilment of the requirements of the degree of

MASTER OF SCIENCE

Department of Electrical and Computer Engineering
University of Manitoba
Winnipeg

Copyright © 2021 by Raghu Ram Atmuri

ABSTRACT

This thesis deals with overvoltages caused due to a ground fault on pole conductor in an overhead bipolar Line Commutated Converter (LCC) HVdc system with a Dedicated Metallic Return (DMR). In HVdc systems with earth return, when a fault occurs, one pole may be lost causing the system to operate in monopolar mode with the ground return. During the fault, overvoltages are induced on the healthy pole resulting in its voltage to increase beyond its rated value. It is already known that these overvoltages reach up to 1.8 pu on the healthy conductor for an HVdc system with ground return due to a ground fault.

Due to large ground currents flow during monopolar operation with ground return, nearby buried metallic structures are subjected to corrosion and these currents might interfere with buried metallic structures. To mitigate the effects caused by a large ground current flowing over a long period, a third Dedicated Metallic Return (DMR) conductor connecting both neutrals of converters, is laid along the line through which the pole current flows. The presence of a third conductor which is grounded only at one terminal and floating on other terminal completely changes the fault mechanics during a ground fault. In this thesis, the overvoltages on the healthy pole and neutral conductors of a dc overhead line with a DMR caused due to a monopolar ground fault are investigated.

Ground faults are applied on a pole conductor at different locations on the line and overvoltages produced along the line are studied. Theoretic explanation of overvoltages is explained based on travelling waves theory and using lattice diagrams. Results showed that overvoltages of up to 2 pu on the healthy pole and 1.2 pu on the dedicated metallic return conductor are observed near the terminal close to ungrounded neutral. It is also observed that the highest overvoltage on the pole conductor occurs due to a fault closer to the ungrounded terminal unlike the case with ground return where maximum overvoltage occurs for a fault at the midpoint.

Keywords: LCC HVdc, dedicated metallic return, ground fault overvoltages.

ACKNOWLEDGEMENTS

The author would like to express his deep gratitude and appreciation to his advisor, Dr. Aniruddha Gole for his constant guidance and support.

The author would like to thank Dr. Athula Rajapakse and Dr. Jenny Zhou for their valuable comments and feedback on the thesis.

The author expresses his love and gratitude to his friends and family who provided immense encouragement and moral support.

Dedicated to my Father

CONTENTS

1 Introduction	1
1.1 Background	1
1.2 Research motivation and objectives	4
1.3 Scope of the project.....	4
1.4 Thesis organization.....	4
2 Overview of HVdc transmission	5
2.1 HVdc transmission system	5
2.1.1 ac system.....	5
2.1.2 LCC converter.....	6
2.1.3 Control system	6
2.1.4 Smoothing reactor and dc filters	9
2.1.5 dc transmission lines	9
2.2 HVdc transmission configurations	10
2.2.1 Back-to-back configuration	10
2.2.2 Monopolar configuration	10
2.2.3 Bipole with ground return.....	11
2.2.4 Bipole with Dedicated Metallic Return (DMR).....	12
2.3 Overvoltages on an overhead dc line	13
2.3.1 Lightning flashovers	14
2.3.2 Insufficient creepages or clearances	15
2.3.3 Switching overvoltages.....	15
2.4 Chapter summary	17
3 Overvoltages on a dc line with ground return	18
3.1 Introduction	18
3.2 Comparison of methodology with previous literature.....	18
3.3 Analysis of overvoltages using lattice diagram.....	22
3.4 Impact of frequency dependent parameters.....	25
3.5 Influence of grid control on overvoltages	28
3.6 Overvoltages for faults along the line	29
3.7 Chapter summary	30

4	Overvoltages on a dc line with dedicated metallic return (DMR)	31
4.1	Introduction	31
4.2	Data used for this study	31
4.3	Influence of grid control on overvoltages	31
4.4	Faults at different locations along the line	34
4.4.1	Difference between a dc line with DMR and a dc line with ground return	38
4.5	Influence of line length on overvoltages	39
4.6	Effect of neutral surge capacitor	40
4.7	Theoretical background	45
4.7.1	Comparison of overvoltages with different neutral grounding and return current path.....	45
4.7.2	Lattice diagram for the case with DMR (i.e., Case 4)	50
4.7.3	Voltage waveforms at other locations (330 km and 990 km) using lattice diagrams	52
4.8	Chapter summary	55
5	Conclusions and future work	56
5.1	Conclusions	56
5.1.1	Observations and conclusions.....	56
5.1.2	Recommendations arising from the research.....	57
5.2	Suggestions for future studies	58
	APPENDIX-A	59
	REFERENCES	60

LIST OF TABLES

Table 3.1 Line parameters used in PSCAD simulations with ground return	20
Table 3.2 Comparison of PSCAD results with previous literature	21
Table 3.3 Comparison of overvoltages waveforms with previous literature	21
Table 3.4 Description of each reflection on lattice diagram	25
Table 3.5 Comparison of voltage waveforms with Bergeron and frequency dependent models.	27
Table 3.6 Comparison of peak overvoltages with Bergeron and frequency dependent models ..	27
Table 4.1 Cases studied for theoretical analysis	45
Table 4.2 Line parameters used for theoretical analysis	46

LIST OF FIGURES

Figure 1.1 Comparison of the right of way requirements for ac and dc transmission [4] (Reprinted with permission of the National Renewable Energy Laboratory)	2
Figure 2.1 Basic structure of an HVdc link	5
Figure 2.2 A 12 pulse converter with two 6 pulse bridges connected in series	6
Figure 2.3 Single line diagram of an HVdc scheme with a constant current controller at rectifier and constant extinction angle controller at the inverter.	7
Figure 2.4 Voltage vs current characteristics of an LCC converter control system	8
Figure 2.5 Champa-Kurukshetra ± 800 kV Tower with two DMR conductors [10].....	10
Figure 2.6 (a) Monopole operating with ground return (b) Monopole operating with the metallic return.	11
Figure 2.7 Bipole operating with ground return	12
Figure 2.8 (a) Bipole with DMR operating in balanced condition (b) Bipole operating in monopolar mode with DMR.	13
Figure 3.1 Naming scheme followed for measuring voltages throughout the thesis.....	20
Figure 3.2 PSCAD schematic for the case with ground return	20
Figure 3.3 Modal voltages at (a) midpoint and (b) terminal, for a fault at the midpoint of a bipolar dc line with ground return	23
Figure 3.4 Voltage vs time graphs for inductive termination	24
Figure 3.5 Lattice diagram for the case with ground return for a fault a midpoint.....	24
Figure 3.6 Variation of (a) surge impedance (b) travel time (c) attenuation, with frequency	26
Figure 3.7 Comparison of healthy pole voltages with and without controls when the line is capacitively terminated. (a) midpoint voltages (b) terminal voltages (NC-no controls, C-controls)	29
Figure 3.8 Overvoltages on a line with ground return for faults along the line.....	30
Figure 4.1 dc triple tuned filter [40] [41]	31
Figure 4.2 Comparison of healthy pole voltages at (a) ungrounded terminal (b) fault point for a fault at the midpoint of line with controls (C) and without controls (NC).....	33
Figure 4.3 Comparison of healthy pole voltages at (a) ungrounded terminal (b) fault point for a fault at 330 km from the ungrounded end, with controls (C) and without controls (NC)....	34

Figure 4.4 dc line with DMR showing five equidistant locations along the line.....	35
Figure 4.5 Voltage vs time graphs for a fault at the midpoint	36
Figure 4.6 Voltage vs time graphs for a fault at 330 km from the ungrounded terminal	37
Figure 4.7 Overvoltages on a line with DMR with faults applied at various locations along the length of the line (1320 km).....	38
Figure 4.8 Overvoltages on a line with DMR with faults applied at various locations along the length of the line (660 km).....	40
Figure 4.9 Comparison of overvoltages along the line with different values of surge capacitor at ungrounded neutral (a) 10 μ F (b) 20 μ F (c) 30 μ F (d) 40 μ F (e) 50 μ F (f) 100 μ F.....	43
Figure 4.10 Impact of surge capacitance value on maximum overvoltage anywhere on the line for faults at any possible locations.....	44
Figure 4.11 Bipolar dc transmission system with fault at the midpoint	47
Figure 4.12 Simulated PSCAD voltages for cases 1 and 2 i.e., without DMR.....	47
Figure 4.13 Simulated PSCAD voltages for cases 3 and 4 i.e., with DMR.....	48
Figure 4.14 Healthy pole voltages on a line with DMR for a fault at midpoint, Case 4	49
Figure 4.15 Lattice diagram for the case with DMR for a fault at the midpoint	51
Figure 4.16 Healthy pole voltages at 330 km and 990 km for a fault at the midpoint of the line with fault resistance of (a) 0.001 Ω (b) 100 Ω	53
Figure 4.17 Lattice diagram showing the voltages at two locations at 330 km and 990 km	54

LIST OF ABBREVIATIONS

ac	alternating current
dc	direct current
DMR	dedicated metallic return
EATL	eastern alberta transmission link
EMT	electromagnetic transient
HVdc	high voltage direct current
LCC	line commutated converter
NESC	national electricity safety code
ROW	right of way
WATL	western alberta transmission link

1 Introduction

1.1 Background

With the rise in commercial usage of electricity in the 19th century the demand to generate more electrical energy from cheaper remote renewable energy sources such as hydro, wind, tidal and so on, has increased. ac transmission is extensively used for transmitting power due to its ease of transformation for different voltage levels and interconnection capability to form a grid. But it has its limitations to transfer substantial amounts of electrical energy over long distances while maintaining stability.

On the other hand, dc transmission had overcome the inherent problems of ac transmission for transferring large amounts of power over long distances without stability issues. The development of manufacturing technology in new solid-state valves (thyristors) from the late 1970s has led to a rapid increase in the application of HVdc transmission [1] [2]. HVdc transmission also possesses advantages over ac transmission including but not limited to (i) interconnecting two asynchronous systems (ii) lower losses compared to the same capacity of an ac line [3] (iii) use of underground or sea cables longer than 30 km (iv) lower right of way requirements for transferring the same power. A comparison showing the right of way requirements for transferring power at different ac and dc voltages is shown in Figure 1.1. As an example, to transmit 6000 MW, at least three 800 kV ac circuits requiring about 183 m (600 ft) ROW compared to two 500 kV dc circuits with 110 m (360 ft) ROW or a single 800 kV dc circuit with 82 m (270 ft) ROW.

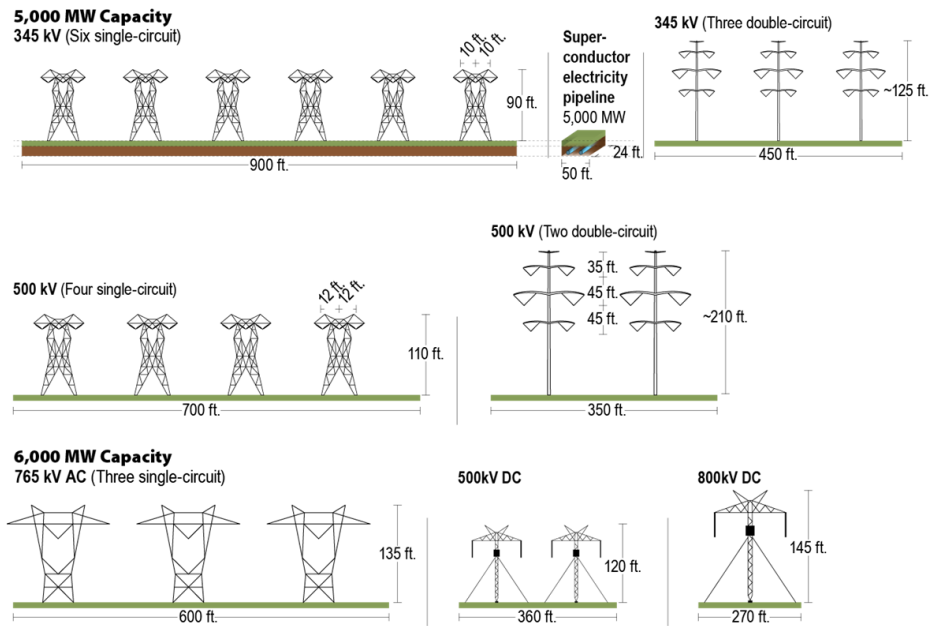


Figure 1.1 Comparison of the right of way requirements for ac and dc transmission [4]
 (Reprinted with permission of the National Renewable Energy Laboratory)

Line Commutated Converter (LCC) HVdc systems which use thyristors as switching device. LCC HVdc is a mature technology; it is well proven and widely used for high power transmission [5] [6]. Most bipolar LCC HVdc projects have ground as the return path due to its advantages in terms of installation cost and line losses [7]. In this mode, the neutrals of both converter stations are grounded through earth electrodes.

When one pole of a bipole is lost or taken out of service (e.g., during maintenance), the dc link can be operated in monopolar mode with the ground return. But operating in earth return mode for long periods may lead to corrosion of buried metallic structures and saturation of nearby transformers core [8] [9]. These drawbacks in earth return operation led to the increased application of Dedicated Metallic Return (DMR) HVdc systems. In this scheme, both converter neutrals are connected through a dedicated neutral conductor along the line and is grounded only at one terminal, through which neutral current flows while poles are unbalanced or during monopolar operation. There are several HVdc projects with DMR as a return path, such as Champa-Kurukshetra [10], Raigarh-Pugulur [11], Quebec-New England, Thailand-Malaysia [12], Eastern Alberta Transmission Link (EATL), Western Alberta Transmission Link (WATL), Hokkaido-Honshu [13] and Kii channel [14]. Due to the problems caused due to flowing of ground currents, continuous use of ground return is not allowed in HVdc applications according to

National Electricity Safety Code (NESC) IEEE standard (Rule 215B5b) [15]. Although the overall cost of the project would increase due to additional conductor along the line, this scheme is still beneficial and today, almost universally mandated, because it eliminates the negative impact of ground currents.

The insulation coordination for an ac overhead transmission line is determined mainly based on switching overvoltages caused by events such as line energization. Since dc systems are energized smoothly by appropriate grid control, the chance of overvoltages due to line energization is minimum [16]. Instead, overvoltage due to ground faults becomes the important criteria for deciding the insulation of a dc overhead transmission line. In an overhead line HVdc system, when a ground fault occurs on one pole, the overvoltage is induced on the healthy pole. When this overvoltage increases beyond the rated insulation value, the healthy conductor might flashover resulting in a bipole outage. So, it is essential to calculate the switching surge factor and design the insulation to withstand these induced overvoltages during fault to avoid bipole outage due to a monopolar fault. In the case of dc overhead line with ground return, it is well known that the switching surge insulation factor is up to 1.8 pu with the highest overvoltages for a fault at the midpoint of the line [16] [17]. Actual field tests conducted on a 1350 km bipolar transmission line support this result [18].

Sometimes when a bipolar dc link needs to be operated in monopolar mode with ground return for longer periods i.e., during maintenance of one pole converter. In this situation, the pole conductor which is not in service can be used as the return conductor which prevents the flow of earth currents [19]. Overvoltages due to ground faults, in this case, are studied and found out that overvoltages will not exceed 1.8 pu on pole conductors [20].

But in the case of dedicated metallic return schemes, the presence of a third conductor which is grounded only at one terminal neutral and floating on another terminal could change the fault mechanics during a ground fault. The effect of this neutral conductor and its effectiveness of fault clearing devices such as arcing horns and neutral grounding breakers is discussed in [21] [22].

1.2 Research motivation and objectives

To the best of the author's knowledge, the published literature regarding overvoltages due to a ground fault on a bipolar dc overhead line with DMR is limited due to its recent application [21] [22] [23]. Taking this into consideration, the following research objectives have been outlined.

- To evaluate the influence of controls on fault overvoltages in the case with a dedicated metallic return.
- To calculate the overvoltages on healthy pole and DMR due to ground faults on pole conductor at various locations along the bipolar line.
- To evaluate the influence of neutral surge capacitor (at ungrounded neutral) on fault overvoltages.
- To provide a qualitative explanation for the overvoltages using lattice diagrams.

1.3 Scope of the project

In this thesis, overvoltages due to only a single pole to ground fault, on a bipolar LCC HVdc overhead line, with a dedicated metallic return are dealt.

1.4 Thesis organization

Chapter 2 provides a brief introduction to HVdc systems and their components. Different schemes of the HVdc system are also explained in this chapter. The various causes of flashovers on an overhead HVdc transmission line such as due to lightning, insufficient creepages and switching overvoltages due to faults were also discussed.

Chapter 3 discusses the phenomenon of overvoltages on a dc line with ground return was explained. Simulations were done to confirm the results of the existing literature and the influence of control systems on overvoltages was also discussed.

Chapter 4 describes overvoltages due to a ground fault at different locations on a line with a DMR conductor. The influence of the control system on these overvoltages was analyzed and conclusions were drawn. The effect of line length on overvoltages and method of reducing these overvoltages is also discussed. The phenomenon of overvoltages on the line with DMR is also described using lattice diagrams.

Chapter 5 presents a summary of the conclusions and suggestions for future works.

2 Overview of HVdc transmission

In this chapter, a brief overview of the LCC HVdc transmission system and its components such as ac system, dc system, Line Commutated Converter (LCC) are discussed. Various operating schemes of dc systems are also reviewed. Different causes of overvoltages on an overhead dc transmission line such as lighting, insufficient creepages and switching overvoltages were also studied.

2.1 HVdc transmission system

Figure 2.1 shows an HVdc link and its main components. The individual components are discussed briefly in the following sections. More detailed descriptions of each component can be found in [1] [24].

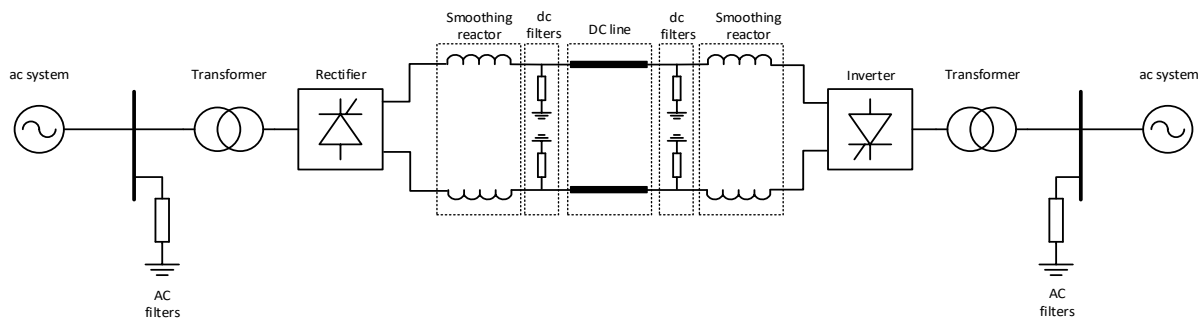


Figure 2.1 Basic structure of an HVdc link

2.1.1 ac system

Typically, a dc transmission system is present as a linkage connecting two ac networks. An ac system mainly consists of ac filters, reactive power compensators, converter transformers and ac switchgear.

Tuned ac filters are installed on the grid side of converter transformers to prevent the penetration of harmonics generated by converters into the ac grid and to provide sufficient reactive power to the converters. Sometimes shunt capacitor banks are also installed in parallel to ac filters to supply reactive power according to the demand of converters.

Converter transformers in the LCC system supply the required ac voltage to the LCC converter by adjusting the taps. Two converter transformers, one Y- Δ and Y-Y are connected in

parallel to each other to one 12 pulse converter, which eliminates lower order harmonics and thus reducing the need for extra filtering equipment on the ac side.

2.1.2 LCC converter

LCC converter is a combination of thyristors arranged in a three-phase full wave bridge known as Graetz Bridge or 6-pulse bridge as shown in Figure 2.2. This converter transforms ac current to dc current at the rectifier and vice versa at the inverter. A detailed overview of LCC converter operation can be found in [24]. Two six pulse bridges are connected series to form one 12 pulse converter. Harmonics are generated from these converters and are injected into both ac network and dc line.

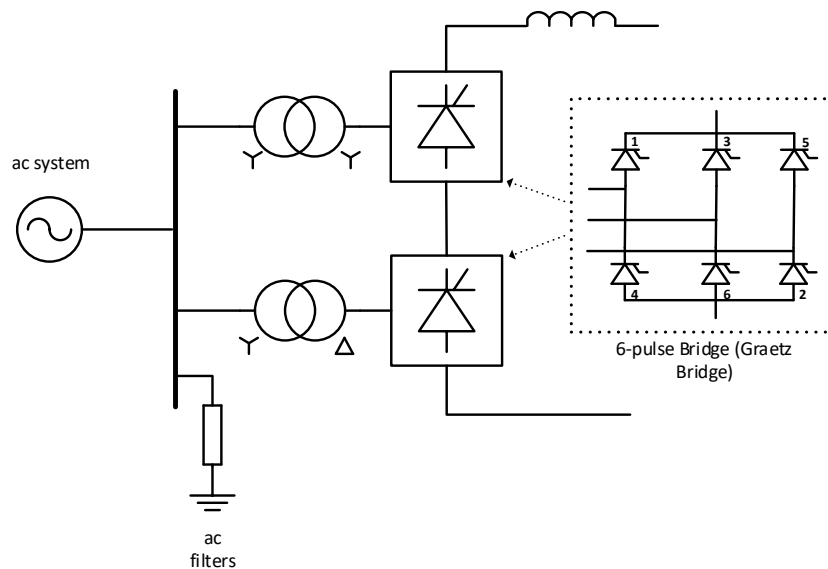


Figure 2.2 A 12 pulse converter with two 6 pulse bridges connected in series

2.1.3 Control system

The firing pulses required to turn on the thyristors are given by the Proportional Integral (PI) controllers, part of closed loop controllers present at both terminals, thereby regulating the power transmitted through the dc link. Figure 2.3 shows a typical control block of an HVdc system. The main control objective of an HVdc link is to transfer maximum power safely according to the load requirement.

The closed loop controls at the rectifier shown in Figure 2.4 result in ABH characteristics, consisting of two line segments namely constant minimum ignition angle, α_0 (CEA) and constant

current, I_d (CC) segment. The closed loop controls at the inverter results in DFG characteristics, consisting of two line segments namely constant extinction angle (γ_0) and constant current (I_d) segment. The difference between the current order at the rectifier and inverter is termed as current margin and is denoted by ΔI_d as shown in Figure 2.4. Under normal operating conditions, the rectifier controls the current while the inverter controls the voltage and bipole operates at operating point E. During a sudden dip in rectifier ac voltage the operating point shifts to L.

For long cable systems, the control modes are reversed, with the inverter assuming current control and the rectifier in constant voltage control [25]. Additional control functions including current error control, voltage dependent current order control, force retard are also present in the control block to improve dynamic characteristics and system performance [24].

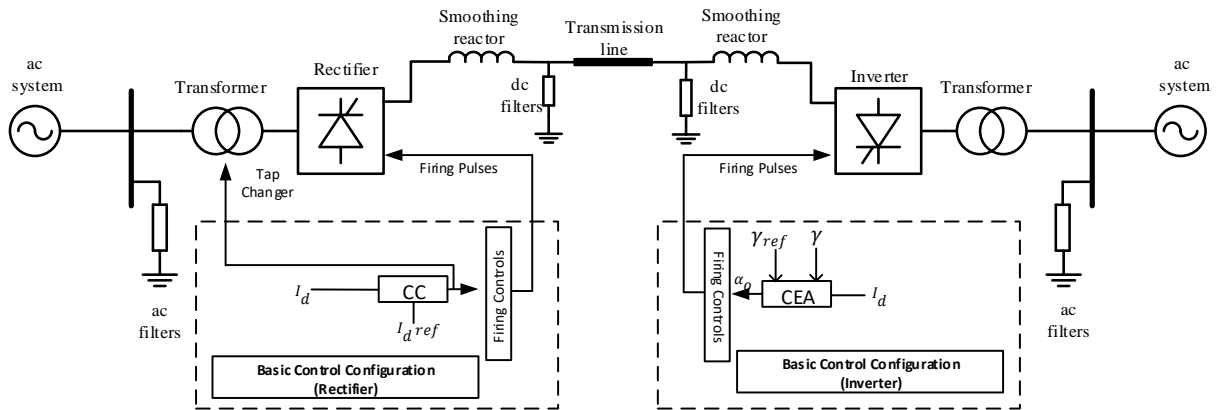


Figure 2.3 Single line diagram of an HVdc scheme with a constant current controller at rectifier and constant extinction angle controller at the inverter.

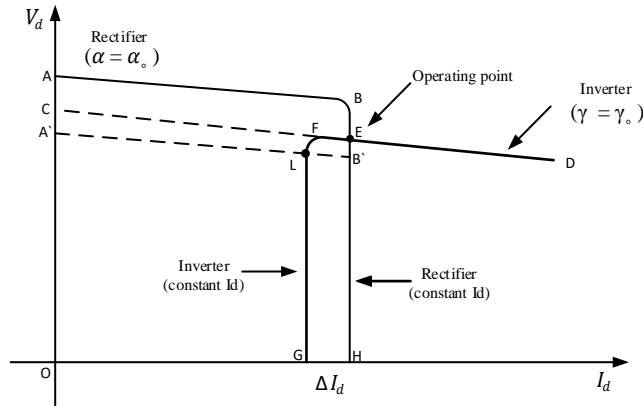


Figure 2.4 Voltage vs current characteristics of an LCC converter control system

2.1.3.1 dc line fault clearing

dc line faults on the transmission lines are detected and differentiated by measuring the voltage and current gradients of travelling waves generated during the fault [26]. Once the fault is identified, they are cleared using force retard operation of the rectifier. In this control operation, the firing angle of the rectifier converter is increased to greater than 90° , thereby enabling it to work in inverter mode and thus discharge the energy on the line, extinguishing the arc. After a certain time delay, the firing angle is slowly brought back to operate in rectifier mode. If the voltage on the line is not restored after this attempt, the fault is assumed to be still existing and force retard action is applied again; if the voltage on the line is not restored after few attempts, the fault is considered to be permanent and requires converter shutdown. It typically takes about 200-300 ms for each force retard attempt, during which the power transfer capability is lost on the faulted pole [27] [28]. During this recovery process, the bipole continues to operate in monopolar mode with either ground or metallic return.

The highest overvoltages due to ground faults are observed within 15 - 20 ms after the fault instant, so, the force retard operation is not considered while calculating the fault overvoltages as it would take a much longer time to confirm the fault and start the force retard sequence.

2.1.4 Smoothing reactor and dc filters

Smoothing reactors are used in series to LCC converters on each pole to limit the sudden rate of change in currents during line faults thereby protecting converter valves.

dc harmonics with frequencies $12n$ where $n = 1,2,3\dots$ are generated by the 12-pulse converter which enters the dc line. If these harmonics are left unfiltered, it might interfere with the communication lines that are present along the line. Therefore, dc filters of dominant harmonics are installed on the dc bus to limit the harmonic content by transferring them to the ground.

2.1.5 dc transmission lines

The rectifier and inverter stations are connected either by overhead transmission lines and/or submarine cables, depending upon the project.

In an overhead transmission line, two pole conductors, ground wires are present along with Dedicated Metallic Return (DMR) conductor depending on the transmission configuration discussed in Section 2.2. Figure 2.5 shows a ± 800 kV dc tower used in the Champa-Kurukshetra project, provided with two DMR conductors along with ground and pole conductors [10].

Ground wires are present on top of the tower, shielding the pole and DMR conductors from lightning. DMR conductors suitably located, could also provide protection to the pole conductors from lightning.

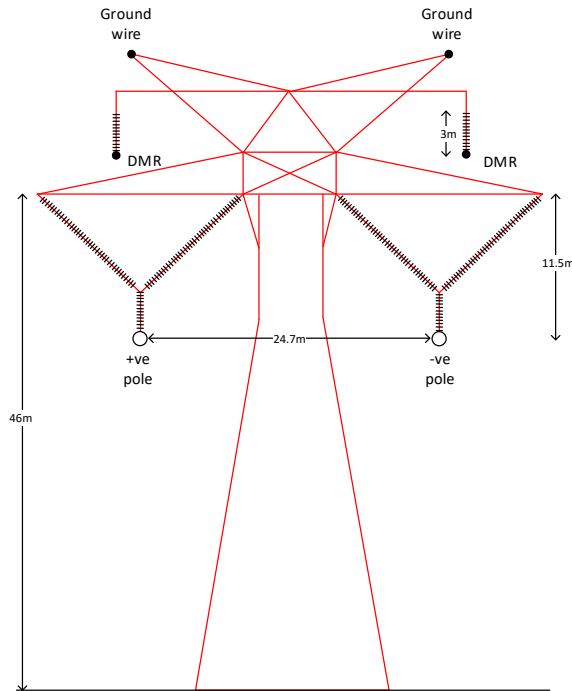


Figure 2.5 Champa-Kurukshetra ± 800 kV Tower with two DMR conductors [10]

2.2 HVdc transmission configurations

HVdc transmission schemes can be broadly classified as explained below.

2.2.1 Back-to-back configuration

In this configuration, the rectifier and inverter are located at the same converter station. Typically, this type of configuration is used to connect two asynchronous ac grids or two weak ac systems to improve their stability. The dc filters are not present and sometimes even the smoothing reactor is not used. This is because both converters are in the same building, and there is no dc transmission line that could create couplings to other ac lines in the neighborhood.

2.2.2 Monopolar configuration

In this configuration, only one pole is used to transfer power and the return path is usually through the ground, or sea in the case of the underground sea cable. Only one conductor is present on the transmission line (for earth or sea return), which not only makes the dc link less expensive but also less reliable, as the entire dc link is compromised when the pole is lost due to any fault. In the case of the metallic return, a conductor grounded at one terminal is present along the line instead of

earth return. A schematic showing a monopolar HVdc scheme with the ground and metallic return options are shown in Figure 2.6 (a) and (b) respectively.

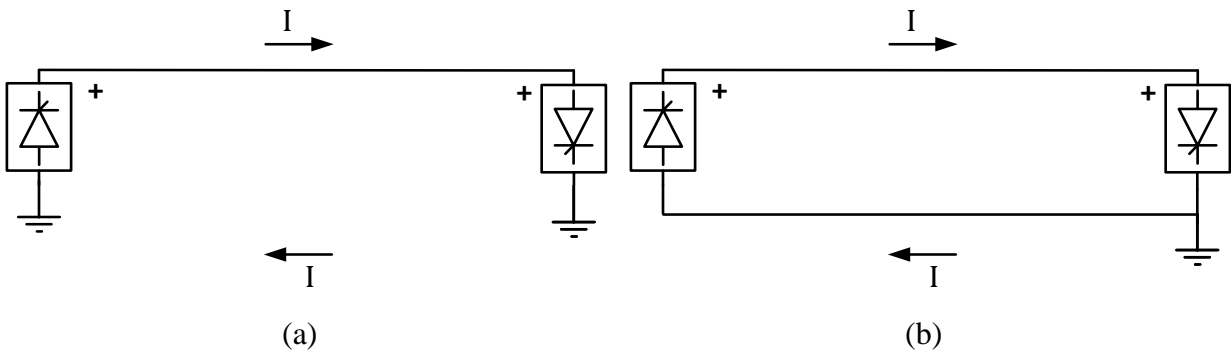


Figure 2.6 (a) Monopole operating with ground return (b) Monopole operating with the metallic return.

2.2.3 Bipole with ground return

Bipolar configuration is a combination of two monopolar systems with a common return path (ground in this case) where one pole has a positive polarity and the other having a negative polarity as shown in Figure 2.7. The power transfer capability is doubled compared to that of the monopolar scheme, and the insulation requirement is reduced due to the maximum voltage to the ground being halved. Another significant advantage of this scheme is when a fault occurs on one pole, instead of losing the entire transmission capacity, the system can be operated usually at reduced capacity, in monopolar mode with ground return.

In this scheme, the neutral points of both terminals are connected to the ground. In normal operating conditions, the unbalanced current in both the poles flows through the ground, except when one pole is taken out for maintenance or during permanent single pole faults, the entire healthy pole current flows through the ground through the neutral point of the converter.

The HVdc station needs a ground reference point for transformers neutral and converter control equipment in the station. This ground reference point at the station is provided by the station ground mat. If the converters neutral point is also connected to the station grounding, the large amounts of dc currents that flow through the station mat increase the ground potential of the ground mat which interferes with the converter equipment affecting the converter performance. To avoid these problems, the converter neutrals are grounded away from the converter stations

(10-50 km) through a special earth electrode. The converter neutral and earth electrode are connected through the electrode line which could be on the same tower as the pole conductors or on a separate tower.

Depending upon the soil resistivity in the area and the rated amperage of the electrode, the ground electrodes may require a large area; could be up to 1 km² [29]. The currents flowing through the ground electrode should not cause any hazards to animals or human beings or cause interference with nearby communication and safety systems. The design of the earth electrode should consider all the safety metrics such as step voltage, touch voltage while satisfying the operational requirements. More details regarding the design of the ground electrodes can be found in [30].

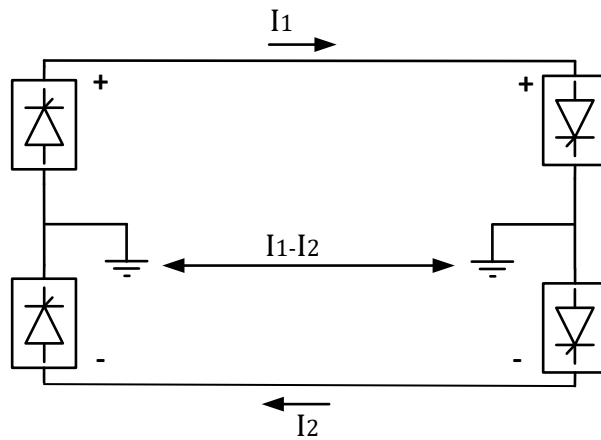


Figure 2.7 Bipole operating with ground return

2.2.4 Bipole with Dedicated Metallic Return (DMR)

Operating the dc link with ground return requires less equipment and has lower line losses due to very low earth resistance. However, operating in this mode may lead to corrosion of buried metallic structures such as gas or oil pipelines, railway tracks, bridges, transmission line towers, etc., [19]. The adverse effects of ground currents were identified in the Talcher-Kolar HVdc system where the ground currents enter the neutral of the transformers present in the vicinity of the electrode, causing core saturation and excessive heat generation [8]. Also, the availability of suitable land for the ground electrode has become a major problem in the present world as it is becoming more difficult to find large areas of suitable land in cities where power demand is more.

To circumvent the issues related to ground electrodes, a metallic conductor is provided for the flow of return current as shown in Figure 2.8. In this configuration, the metallic return conductor, called Dedicated Metallic Return (DMR), strung on the same tower as the pole conductors, grounded only at one terminal, provides the return path for current. The steady state insulation required for a DMR conductor is typically low compared to the pole conductor, depending on the voltage for which it is rated to operate during the monopolar mode.

Although DMR conductor solves the problems caused by flowing ground currents, it also possesses drawbacks including but not limited to

- Increased initial and operating cost due to additional conductors and higher DMR resistance.
- Increased probability of back flashover on the line, especially onto DMR conductors due to their closeness to the tower's metallic structure. This underscores the necessity for DMR fault clearing protection [21] [22].

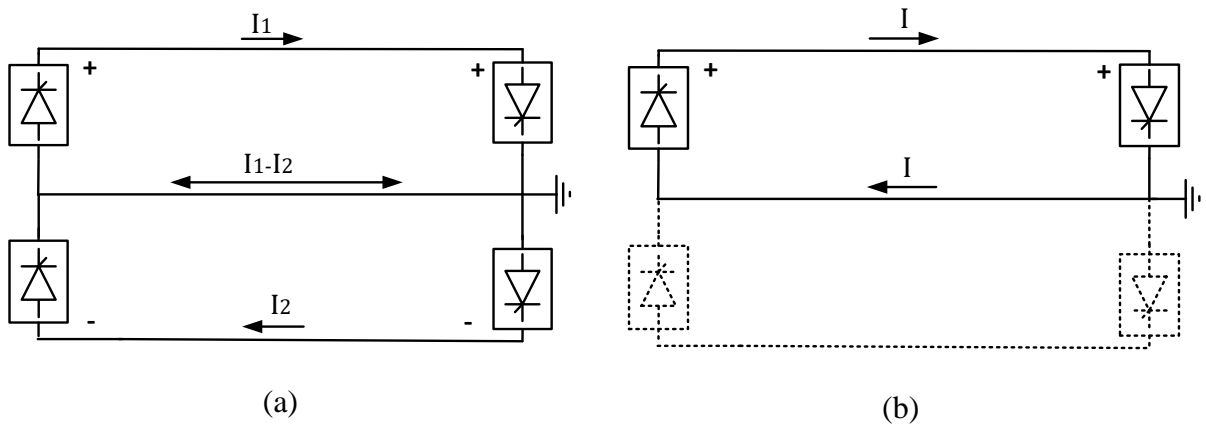


Figure 2.8 (a) Bipole with DMR operating in balanced condition (b) Bipole operating in monopolar mode with DMR.

2.3 Overvoltages on an overhead dc line

An overhead transmission line is designed to operate for certain voltage conditions which are calculated based on many factors such as internal overvoltages, lightning overvoltages and normal operating voltage. The first two factors impose requirements mainly on the insulator string length and air gap distances, while the latter influences the selection of leakage distance of insulator units

and hence the string length especially when contamination conditions exist [16]. If the voltage on the line exceeds its designed rated voltage, flashover can happen which results in loss of the ability to transfer power on the faulted pole. The main goal of insulation coordination is to estimate the minimum required insulation level where the possibility of flashover can be minimized to a certain acceptable risk of failure.

In this section, the factors such as switching overvoltages, lightning overvoltages and steady state voltages which influence the dc overhead line insulation coordination are explained briefly.

2.3.1 Lightning flashovers

Lightning is one of the common causes of flashovers on an overhead transmission line. Flashovers on a transmission line can happen due to lightning strikes in two ways.

2.3.1.1 Shielding failure

An overhead transmission line is protected from lightning flashes by ground wires which are present on top of the tower, along the length of the transmission line. These ground wires act as a shield by absorbing the lightning energy and diverting them to the ground, thereby protecting the pole conductors.

If adequate shielding is not provided, lightning might strike the pole conductor which increases the voltage on the conductor beyond its withstand value, resulting in flashover across the insulator (arc from conductor to tower).

2.3.1.2 Back flashover

When lightning hits the ground wire or metallic parts of the tower, depending on the value of the tower footing resistance and lightning stroke current, a voltage greater than the insulation withstand voltage might be generated across the insulator string or air gap (between conductor to tower), resulting in a flashover. In this case, the arc travels from the tower body to the conductor and hence, this phenomenon is called a back flashover.

In the case with bipolar dc line, it should be considered that the operating voltages on each pole are of opposite polarity. When lightning hits the ground wire, the cross arm will experience a voltage that will be of the same polarity of one pole and opposite to another. Since most of the

lightning strokes are of negative polarity, the flashover of the positive pole would occur before the negative pole flashover [16]. The lightning performance of a dc line is similar to that of an ac line except that this biasing effect should be considered for dc lines. The insulation of a dc line is mainly dictated by internal overvoltages and steady state voltages rather than lightning voltages except for low voltage dc lines and areas with high isokeraunic levels.

Irrespective of shielding failure flashover or back flashover, they result in a ground fault.

2.3.2 Insufficient creepages or clearances

Creepage is the shortest distance measured along the surface of the insulating parts of the insulator expressed in mm/kV. Due to pollution and other contaminants such as sand, ice, snow, dew, bird droppings etc., which might deposit on the surface of the insulating material, reducing the strength of the insulation which could result in a flashover during steady state operating conditions.

2.3.3 Switching overvoltages

2.3.3.1 Overvoltages during line energization

Unlike an ac line, a dc line is energized smoothly by appropriate grid control of the firing angle of thyristor valves resulting in negligible overvoltages during line energization.

2.3.3.2 Overvoltages due to line faults

Ground faults can happen on a transmission line due to several reasons. It can happen during steady state conditions when there is no sufficient creepage or it can happen when conductors touch nearby objects such as trees. Since the largest internal overvoltages are produced due to monopolar fault to ground, there is a necessity to calculate these overvoltages and design the insulation to withstand these overvoltages [31].

2.3.3.3 Pole-Pole faults

Pole to pole faults on a dc line are highly unlikely to occur as two poles of a bipole are physically separated with large clearances. If both poles are involved in the faults such as pole-pole fault or double pole-ground faults, force retard is applied on both the poles and power transfer capability is restored after force retard is finished. During this time, the entire dc link is compromised.

2.3.3.4 DMR faults

Since the DMR conductor is grounded at one end, a fault between pole and DMR is technically a pole to ground fault but with high fault resistance.

During balanced operation, a ground fault on the DMR conductor will not necessarily lead to a pole outage, as there is no adequate voltage on the DMR to maintain the arc. But when a DMR fault occurs during monopolar operation or unbalanced bipolar operation, with currents flowing through the DMR, the arc could be sustained for long periods of time by the DMR current, damaging the insulation and create a potential hazard. So, it is necessary to identify and clear the faults on DMR. A fault protection sequence for the ± 500 kV, Kii channel HVdc system is discussed in [32].

A study was conducted on Quebec-New England HVdc intertie to analyze the overvoltages and provide methods to clear DMR faults [22]. These methods include, such as to increase the insulator units on both pole and DMR to prevent simultaneous faults, or temporarily interrupting the pole currents to extinguish the arc on DMR or installing arcing horns on DMR insulators to extinguish the arc. But a conclusion is made to install a high-speed ground switch at the ungrounded end to temporarily operate the system with ground return which extinguishes the arc. In ± 300 kV, 110 km Thailand-Malaysia project, arcing horns were provided on DMR conductors along with high speed ground switch at the ungrounded end [12]. A similar study discussing the efficiency of arcing horns to clear faults on DMR conductor can also be found in [21].

2.3.3.5 Pole-Ground faults

In a dc line, the largest internal overvoltages are produced due to monopolar fault to the ground [31]. When a single pole-ground fault happens on a bipolar line, the power transfer capability of the faulted pole is lost, and the system operates in monopolar mode with either ground or metallic return. As two poles are within close proximity, they influence each other during transient conditions through electromagnetic and electrostatic coupling. Voltages on the faulted pole are induced on the healthy pole at the time of fault and could increase the voltage on the healthy pole to beyond its rated voltage resulting in a flashover of the healthy pole causing an entire bipole shutdown disregarding the purpose of bipole. Thus, the insulation of a bipolar dc line should be designed in such a way so that, the fault on one pole should not lead to a bipole outage.

In this thesis, the study of overvoltages due to pole-ground fault on a dc overhead transmission line especially with a dedicated metallic return is performed.

2.4 Chapter summary

In this chapter, a brief overview of an LCC HVdc system along with its main components are discussed. Classification of dc schemes based on the arrangement of 12-pulse converters and neutral current path are discussed.

The main causes of overvoltages on a dc overhead line such as lightning, insufficient creepages and switching overvoltages are reviewed. Different types of faults on a dc overhead line are identified and discussed. The necessity of calculating overvoltages during a single pole to ground fault is identified.

3 Overvoltages on a dc line with ground return

3.1 Introduction

The phenomenon of ground fault overvoltages on a dc line with ground return, neutrals of each converter station are grounded, is explained by Kimbark using travelling wave theory [33]. When a fault occurs on one pole, travelling waves with positive and zero sequence components are produced on the healthy pole at the fault point and travel in both directions of the line towards terminals. The waves reflect at the terminals with a magnitude depending on the terminal impedance and meet at the fault point producing peak overvoltages at the centre. It should be noted for this case that maximum overvoltages occur at the location of fault due to first reflections of sequence components reflecting at terminals and meeting at the location of the fault. These overvoltages are simulated using a digital program by Hingorani for various line terminations [34].

According to Hingorani, a short circuit between a pole and ground on an overhead bipolar dc transmission line can produce overvoltages on the healthy pole that could result in bipole outage. These magnitudes of overvoltages depends on various factors including,

- Location of fault on the line
- Line attenuation
- Type of line termination

It should be considered that Hingorani and Kimbark's work had ignored the frequency dependency of zero and positive sequence waves in their work. Studies were conducted for different lengths of lines considering frequency dependency of line parameters and observed that maximum overvoltages up to 1.8 pu can happen when a fault occurs at the midpoint of the line [17]. The results of the actual field tests conducted on a 1350 km dc line by Melvold et.al revealed that the actual line overvoltages are lower than the simulated values which are due to inaccuracies in modelling the frequency dependency of sequence components [18].

3.2 Comparison of methodology with previous literature

Before calculating the overvoltages on a dc line with a metallic return, a model of the dc line with ground return was constructed and simulated on PSCAD/EMTDC and the results were compared with existing literature [34] to verify methodology.

The PSCAD model is for a ± 500 kV, bipolar HVdc system with ground return with transmission line parameters as those of Hingorani [34]. The transmission line modelled is 1320 km long with tower dimensions as in [35].

Initially, a lossless Bergeron model [36] is used to model the transmission line, which calculates the line constants only at a single frequency (here 200 Hz). In the original Bergeron model, the line is considered completely lossless (i.e., zero conductor and ground resistivities). This also gives equal travel times for positive and negative modes. However, if ground resistivity is included, the travel times are different. Hence this modified Bergeron model is used in which different travel times and sequence surge impedance values are specified. This was done by Hingorani with line parameters as given in Table 3.1 and the author's initial simulations. This was done so that results could be compared with the Hingorani model to validate the basic approach. Later in the thesis, a fully frequency dependent J Marti model [37], which considers the line constants at various frequencies was used for more accuracy and also for seeing the effect of including more detail.

The converters were represented as dc sources, i.e., the influence of controls was not included. A smoothing reactor of 0.5 H was present on each pole at both rectifier and inverter as shown in Figure 3.2. Two different line terminations were studied as suggested by Hingorani.

- With only a smoothing reactor of 0.5 H - Inductive termination
- With a 0.7 μ F capacitor on each pole in addition to the 0.5 H reactor – The capacitive termination crudely takes into the effect of a dc filter or surge capacitor as shown in Figure 3.2. This is referred to as “Capacitive termination” in the thesis.

The following convention is used to refer to node voltages at different locations on the dc line in this thesis can be found in Figure 3.1.

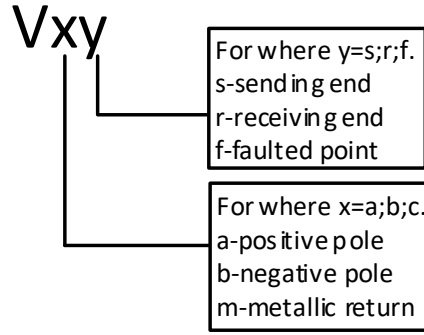


Figure 3.1 Naming scheme followed for measuring voltages throughout the thesis

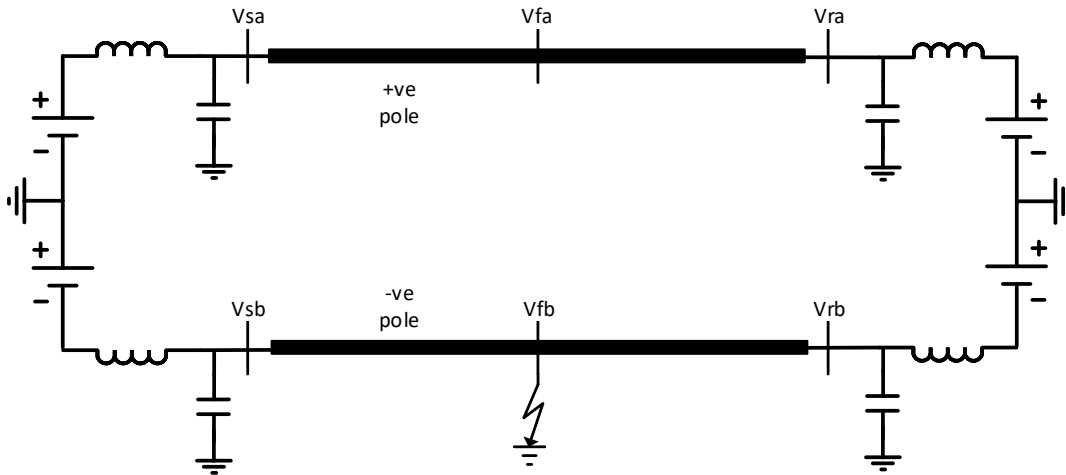


Figure 3.2 PSCAD schematic for the case with ground return

Table 3.1 Line parameters used in PSCAD simulations with ground return

Line parameters (at 200 Hz)	Positive sequence parameters	Zero sequence parameters
Impedance (Z), in Ω	281	507
Travel time for the full length of line (T) in ms	4.38	5.82

With the parameters mentioned in Table 3.1, a solid ground fault (i.e., zero fault resistance) was applied on the negative pole at the midpoint of the line for each line termination. The peak overvoltages on the healthy pole at both midpoint and terminals were measured. Since both

neutrals of converters are grounded, the reflections of travelling waves at both terminals will be symmetrical, so, only the voltages at one terminal were presented in Table 3.2 and Table 3.3.

Table 3.2 Comparison of PSCAD results with previous literature

Healthy pole voltages at	Hingorani * [34] (pu)	EMT Model * Bergeron Model (pu)	EMT Model FD model (pu)
For inductive termination			
Midpoint	2.35	2.3	1.5
Terminal	1.8	1.8	1.1
For capacitive termination			
Midpoint	2	2.1	1.85
Terminal	1.5	1.5	1.2
* Values calculated with Bergeron model at 200 Hz			

Table 3.3 Comparison of overvoltages waveforms with previous literature

	Inductive termination	Capacitive termination
Hingorani results [34]	<p>Fig. 3. Voltages on positive pole for midpoint fault on negative pole; dc reactor termination.</p>	<p>Fig. 5. Voltages on positive pole for midpoint fault on negative pole; capacitive termination to waveroft.</p>
EMT Simulation results (Bergeron at 200 Hz)	<p>Healthy pole terminal voltages</p>	<p>Healthy pole terminal voltages</p>

For the Bergeron model, the maximum voltages at midpoint and terminal for inductive termination were found to be 2.3 pu and 1.8 pu, respectively. In addition, when the surge capacitor was used at the terminal, the terminal voltage has been reduced from 1.8 pu to 1.5 pu. The results obtained were in close agreement with the results of Hingorani.

3.3 Analysis of overvoltages using lattice diagram

The phenomena of travelling waves can be used to understand the concept of overvoltages due to a fault. The waveforms observed in Table 3.3 can be understood using such an approach. As the coupled bipolar dc line with ground has two conductors and a ground path, the voltages and currents can be resolved into two decoupled modal components – an aerial mode and a ground mode. In the prevailing literature in this field [33] [38], they are also referred to respectively as the positive sequence and zero sequence modes, which is the terminology followed in this thesis. Travelling waves of these two modes are produced at the fault location and travel towards the terminals at two different velocities with the positive sequence wave travelling faster than the zero sequence wave. Kimbark [33] first proposed a qualitative explanation to rationalize the relative overvoltage magnitudes and the times at which they occur.

The reflections of these travelling waves can be easily illustrated using a lattice diagram. A lattice diagram as in Figure 3.5, shows the reflections of travelling waves for the ground fault at the midpoint of the bipolar dc line with a ground return. The horizontal axis and vertical axis represent the distance between the terminals and the time originating from fault instant, respectively. The travelling waves in both modes are represented as straight lines with a slope depending on the velocity of the travelling wave for each mode. The positive and zero sequence waves are represented in solid and dashed lines respectively in the lattice diagram. At the point of discontinuity (terminals and fault location), these waves get reflected and transmitted. For a fault at the midpoint of dc line with ground return, the reflections of these waves are symmetrical along the midpoint.

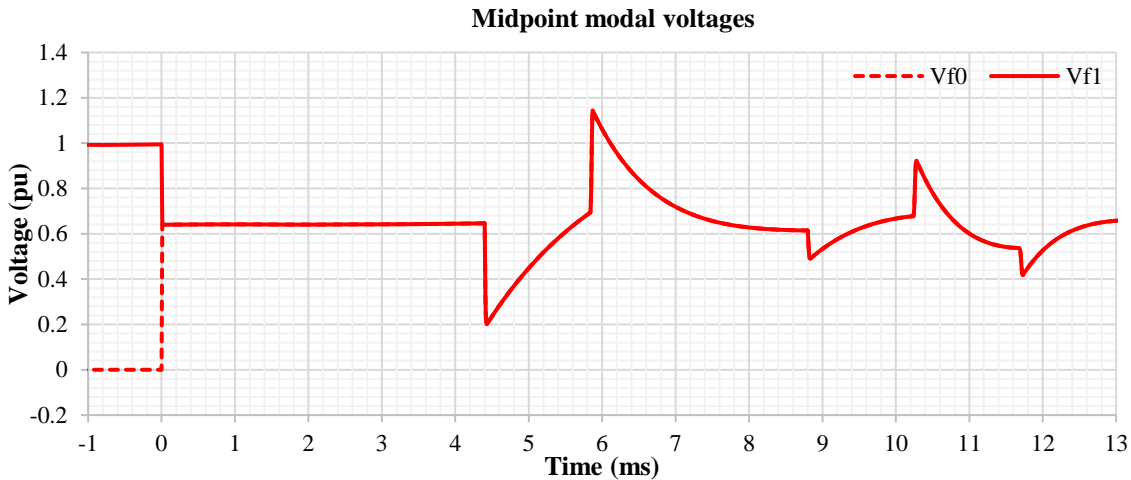
The time instants of discontinuity of these waves at midpoint and terminals are designated as A, B, C... and 1, 2, 3... respectively in Figure 3.4 and Figure 3.5. In Figure 3.4, the overvoltages as a function of time are shown for a fault at midpoint with inductive termination, with the same designation as represented above. Parameters used for this inductive termination are shown in

Table 3.1. Note that Figure 3.4 is essentially the same as the figure in Table 3.3 for inductive termination.

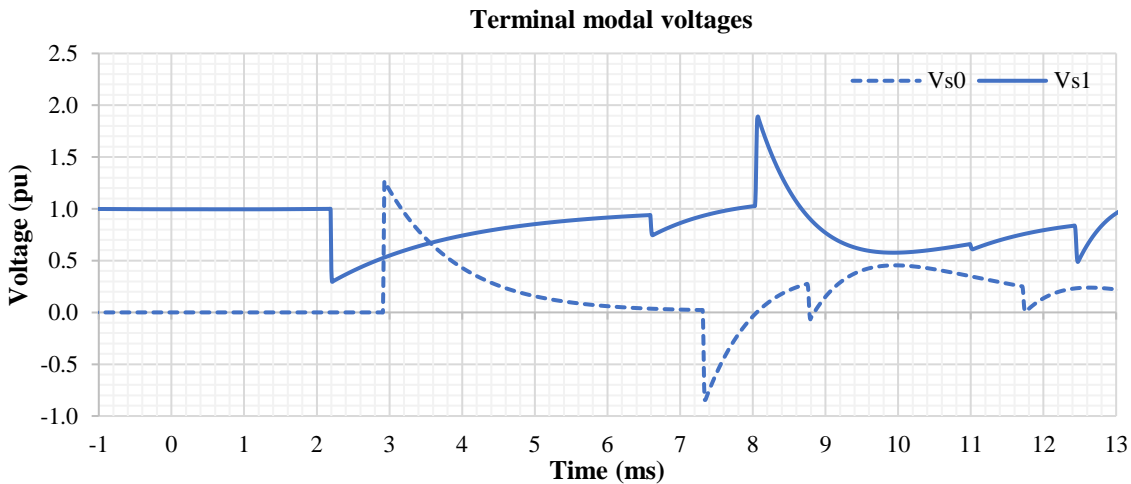
The positive and zero sequence modal voltages, V_1 and V_0 and can be calculated by the formulae given by Kimbark [33] and is shown in Equation 3.1. These modal waveforms are calculated for the voltages at both midpoint and terminal and are plotted in Figure 3.3.

$$V_0 = \frac{V_a + V_b}{2} \qquad V_1 = \frac{V_a - V_b}{2} \qquad \dots\dots\dots (3.1)$$

where V_a and V_b are the positive and negative pole voltages



(a)



(b)

Figure 3.3 Modal voltages at (a) midpoint and (b) terminal, for a fault at the midpoint of a bipolar dc line with ground return

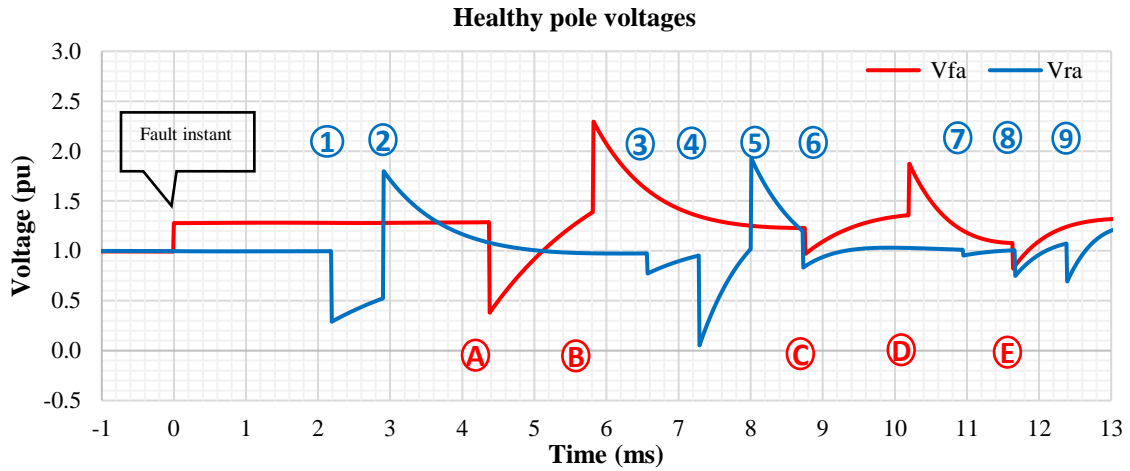


Figure 3.4 Voltage vs time graphs for inductive termination

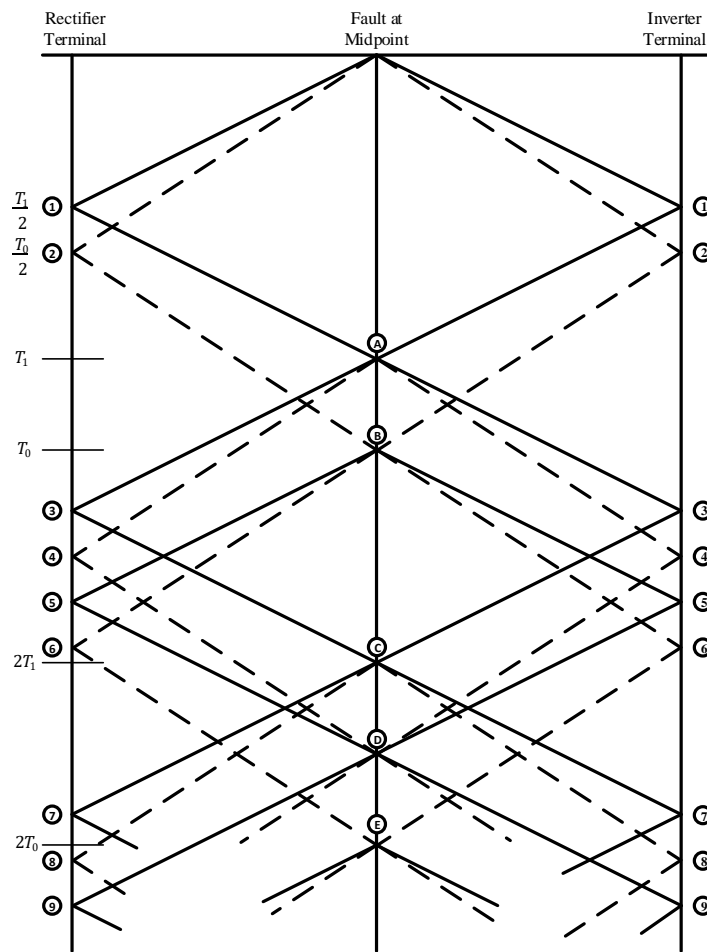


Figure 3.5 Lattice diagram for the case with ground return for a fault a midpoint

In Table 3.4, an explanation is given for each point on the lattice diagram and voltage vs time graphs.

Table 3.4 Description of each reflection on lattice diagram

Designation	Description	Time from fault instant
1	Positive sequence wave reaches the terminal	$\frac{T_1}{2}$
2	Zero sequence wave reaches the terminal	$\frac{T_0}{2}$
A	Positive sequence wave returns to midpoint	T_1
B	Zero sequence wave returns to midpoint	T_0
3	Positive sequence wave returns to the terminal after reflection at the midpoint	$\frac{3T_1}{2}$
4	Zero sequence refracted wave at instant A reaches to terminal	$T_1 + \frac{T_0}{2}$
5	Positive sequence refracted wave at instant B reaches to terminal	$T_0 + \frac{T_1}{2}$
6	Zero sequence wave reflected at instant B reaches to terminal	$\frac{3T_0}{2}$

3.4 Impact of frequency dependent parameters

If the line and ground resistivities are small, then the transmission line parameters (e.g., L and C per unit length) can be approximated as constants. However, in real transmission lines, the ground resistivity, in particular, makes the parameters frequency dependent and changes surge impedance, travel times and attenuation of the positive and zero sequence modes also frequency dependent. For the above transmission line, the surge impedance, attenuation, and travel times at various frequencies are shown in Figure 3.6. Note that the frequencies are highly attenuated at a higher frequency, and as a result, would reduce the sharp peaks in the waveform. Also, the constructive and destructive interference times between the modes would vary from that in the lossless case, thereby modifying the times at which the peaks occur. Repeating the simulation case in Section 3.2 with frequency dependent model gives the results in Table 3.5 and Table 3.6. It can be seen that the peak overvoltages at midpoint and terminal are much lower with the frequency

dependent model, indicating that the analysis from previous research is too pessimistic. At the time of Kimbark's research, the state of the art of modelling transmission lines in the time domain was in its infancy, and so the Bergeron model was used. However, now that improved models are available, the topic can be revisited with more accurate modelling.

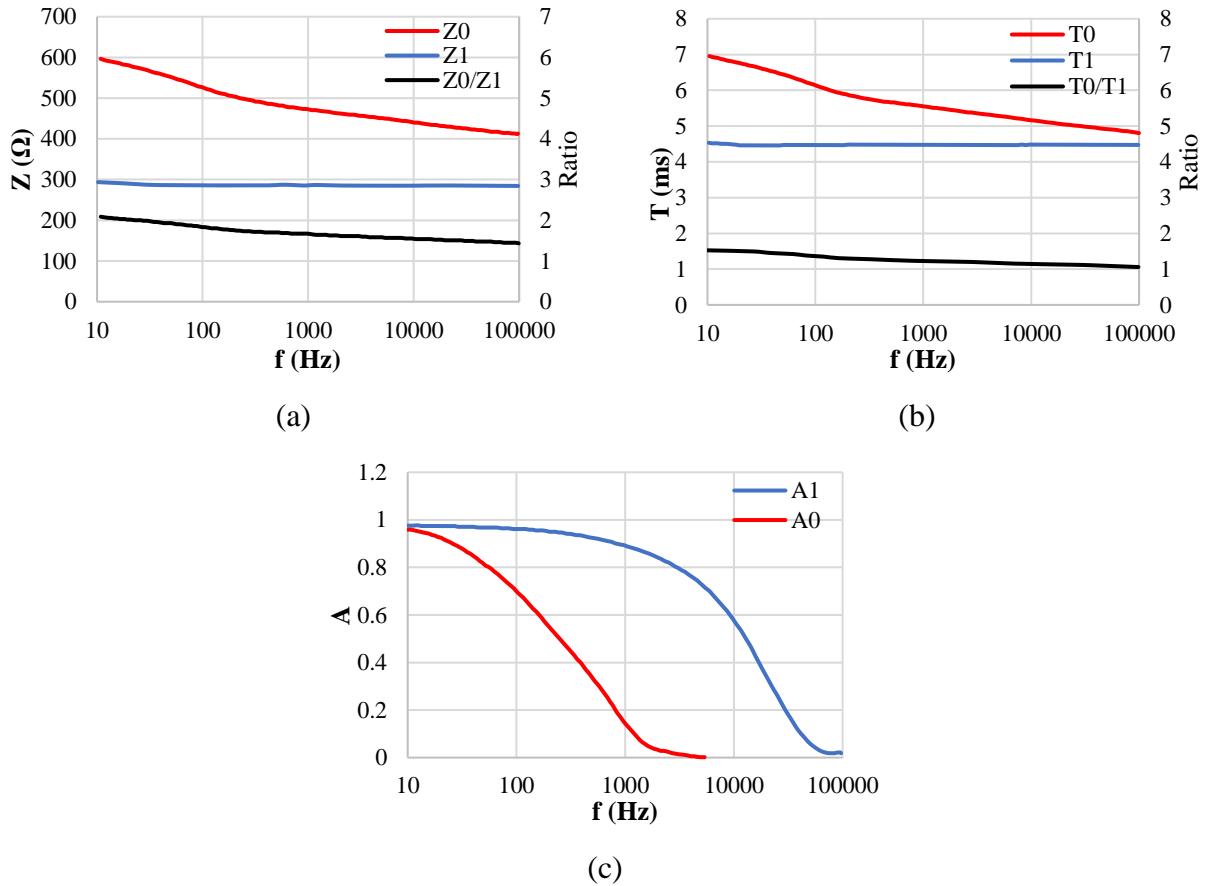


Figure 3.6 Variation of (a) surge impedance (b) travel time (c) attenuation, with frequency

Table 3.5 Comparison of voltage waveforms with Bergeron and frequency dependent models

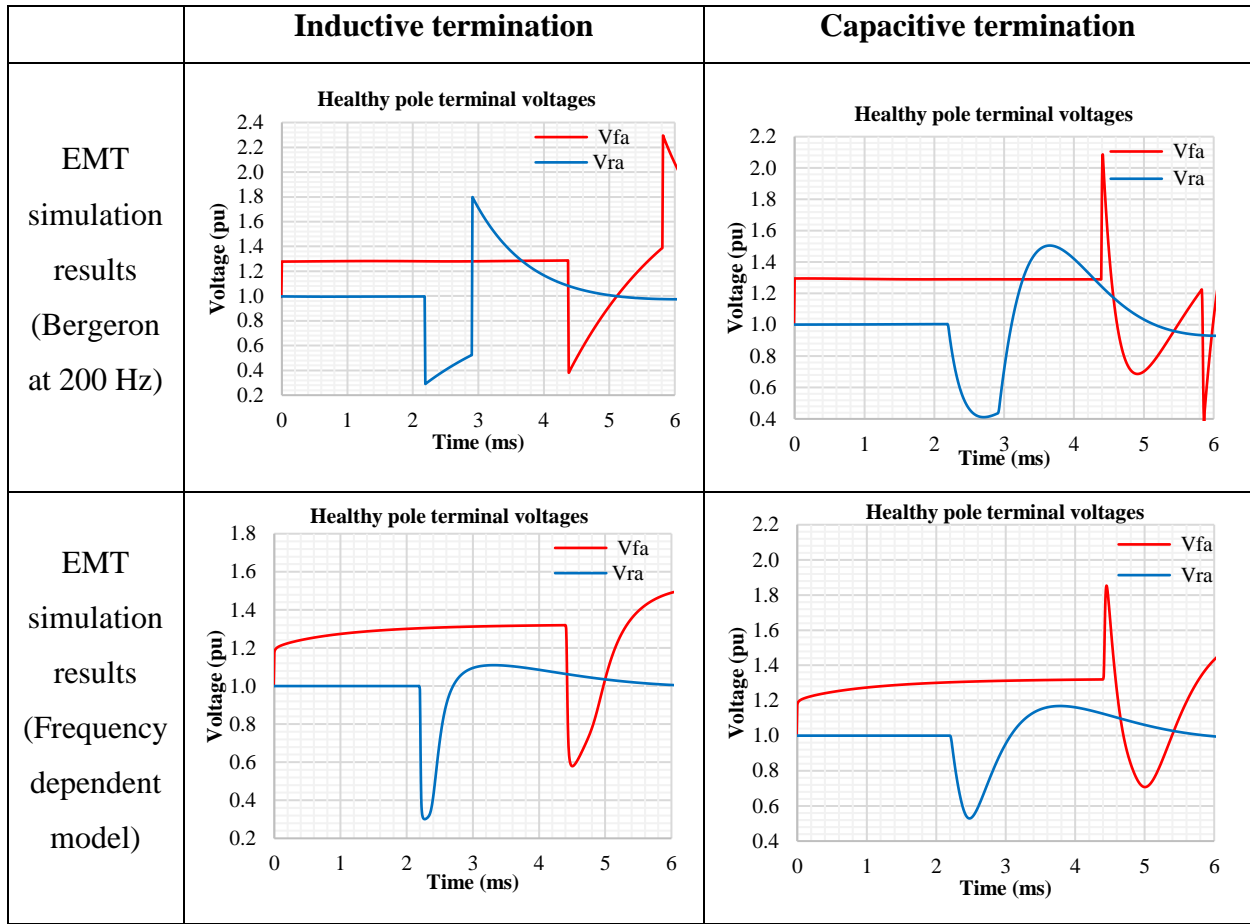


Table 3.6 Comparison of peak overvoltages with Bergeron and frequency dependent models

Healthy pole voltages at	EMT Model Bergeron Model (pu)	EMT Model FD model (pu)
For inductive termination		
Midpoint	2.3	1.5
Terminal	1.8	1.1
For capacitive termination		
Midpoint	2.1	1.85
Terminal	1.5	1.2

3.5 Influence of grid control on overvoltages

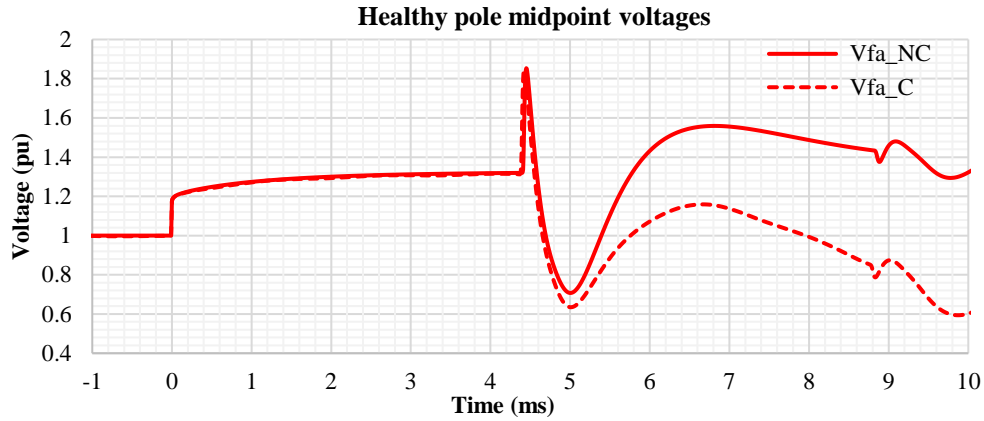
As discussed in Section 2.1.3, controls of the LCC HVdc system are intended to maintain the voltage and the current in dc link to maintain the optimum power. After the fault, the travelling waves change the terminal voltage and the current, which in turn leads to the change in the firing angle of the converter to maintain the nominal voltage and current on the line, by the controllers.

According to Hingorani, if the line is capacitively terminated, the maximum overvoltages are caused due to the first reflection of the positive sequence wave. It was felt that the travelling waves would leave the terminal towards the midpoint before the controller changes its firing angle and so the controller would not affect the first overvoltage peak. Hingorani confirmed this with a simplified controller model in the simulation. However, his paper suggested considering the influence of controls when a line is terminated other than capacitively.

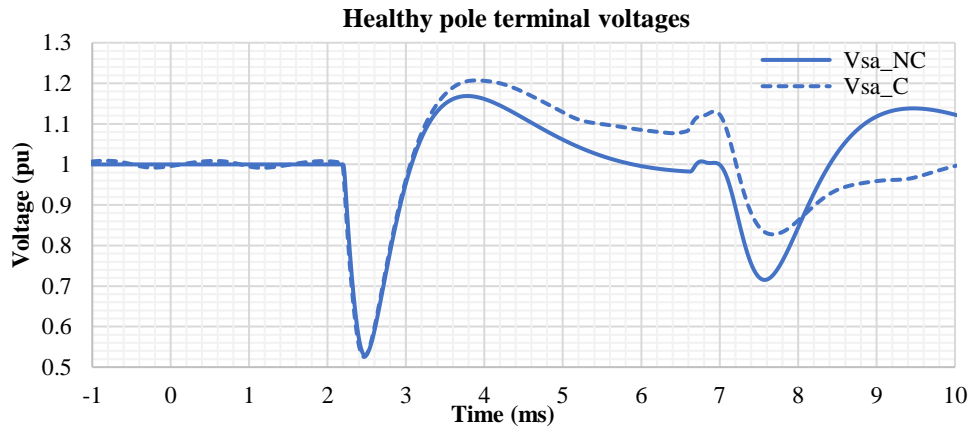
Since Hingorani has indicated that there is no significant influence of grid control on the magnitude of overvoltages for capacitive termination, CIGRE benchmark controls [39] have been incorporated in this work, to confirm the work of Hingorani.

Frequency dependent model with transmission line dimensions, as adopted in Section 3.2 were used with line capacitively terminated. A ground fault with negligible fault resistance was applied on the negative pole at the midpoint in both cases, i.e., with and without controls. The voltages of the healthy pole at the midpoint and terminal of the line are compared with both the cases and are plotted in Figure 3.7.

The results showed that the presence of controls has no effect on the peak voltages at both midpoint and terminals. This is because the peak overvoltages, in this case, occur due to positive sequence reflections and the highest peak voltage is observed before the control action reduced the overvoltage. However, later the voltages in the case with controls are kept lower by the action of controls compared to the other case, confirming the Hingorani results.



(a)



(b)

Figure 3.7 Comparison of healthy pole voltages with and without controls when the line is capacitively terminated. (a) midpoint voltages (b) terminal voltages (NC-no controls, C-controls)

3.6 Overvoltages for faults along the line

Previous research has shown that the maximum overvoltages on a dc line with ground return for a ground fault occur for a fault at the midpoint of the line [17] [34]. In this section, faults are applied along a 1320 km line with system parameters as used later in Section 4.2 except that the system uses a ground return instead of the DMR conductor. Ground faults with zero resistance are applied on the negative pole at five equidistant locations on the line which are 330 km apart from each other. The results are plotted in Figure 3.8, which confirm that the highest overvoltage of 1.8 pu for a fault at the midpoint and with decreasing overvoltage towards the terminal ends of the line. These results are a baseline that will be compared later in section 4.4. with the overvoltages on a dc line which uses a DMR conductor.

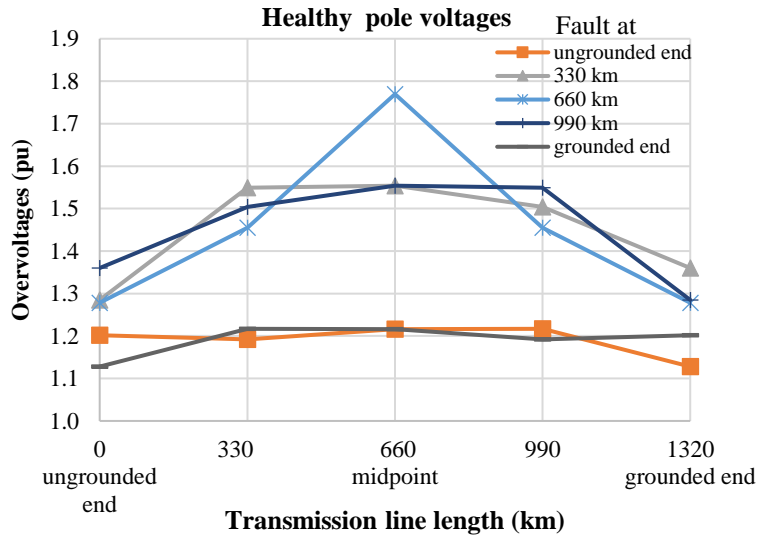


Figure 3.8 Overvoltages on a line with ground return for faults along the line

3.7 Chapter summary

In this chapter, the phenomena of overvoltages on a dc line with ground return have been studied mainly using EMT simulation. A qualitative explanation based on travelling wave theory and lattice diagram was also given. The overvoltages on a dc line with ground return caused due to ground faults remain below 1.8 pu with maximum overvoltages for a fault at the midpoint of the line. The impact of using a particular line model was also investigated. The more accurate frequency dependent model was shown to give a lower overvoltage estimate and hence was recommended for further study.

The effect of grid control on overvoltages is negligible as peak overvoltages happen due to the first reflections of travelling waves. EMT simulations were also done to validate the methodology of modelling and influence of controls on overvoltages with reference to published literature.

4 Overvoltages on a dc line with dedicated metallic return (DMR)

4.1 Introduction

In this chapter, the overvoltages induced on the healthy pole and DMR conductor are evaluated due to a pole to ground fault applied on one pole at various locations along the line for the given ± 800 kV bipolar line with DMR which is grounded at the inverter end. The influence of converter controls is evaluated in finding the overvoltages. A lattice diagram showing the reflections of travelling waves is discussed for getting a qualitative understanding.

4.2 Data used for this study

The transmission line represented is 1320 km, 800 kV tower with two hexagonal lapwing pole conductors, one quad lapwing DMR conductor (grounded at inverter terminal) and two ground wires. The tower and conductor dimensions are given in Appendix-A. A 0.5 H smoothing reactor is present on each pole at both ends of the line. A triple tuned filter (12,24,36th harmonic filter-50 Hz) from which is capacitive to incoming surge is present. The filter data is as given in [40] [41]. The triple tuned filter configuration is shown in Figure 4.1.

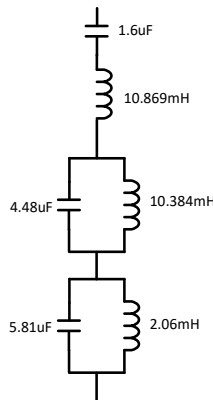


Figure 4.1 dc triple tuned filter used in simulations [40] [41]

4.3 Influence of grid control on overvoltages

The influence of grid control on overvoltages is discussed by Hingorani for the case with the ground return [34]. As discussed in Chapter 3, the presence of grid controls does not affect the peak overvoltages on the dc line with the ground return. EMT simulation results indicating the same were discussed in Section 3.5. However, no such information is available in the literature, for the case with a dedicated metallic return. To understand the influence of grid control for the

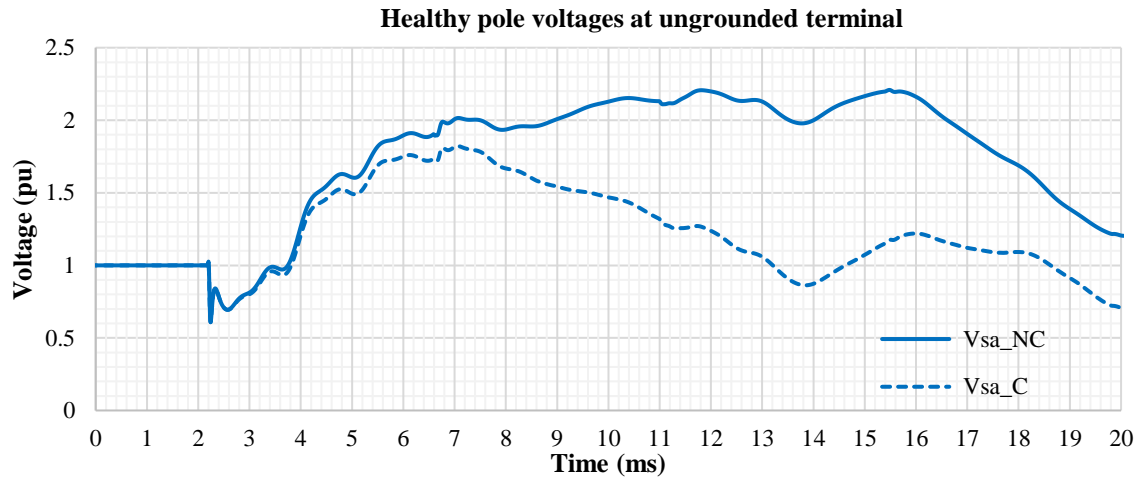
case with DMR, two PSCAD models, with and without controls, of an HVdc system with DMR are studied. By comparing the results of both cases, the influence of controls can be identified.

In the case without controls converters are represented as a dc source with data mentioned in Section 4.2. CIGRE benchmark controls are used for the case with controls [39]. A frequency dependent model is used in PSCAD to model the transmission line. A ground fault is applied on the negative pole at two locations on the line, midpoint and at a point that is 330 km away from the ungrounded terminal. The healthy pole voltages at the fault point and ungrounded terminal are measured against time for both the fault cases i.e., at the midpoint and 330 km point and are presented in Figure 4.2 and Figure 4.3 respectively. The naming convention used to refer to node voltages at different locations on the dc line can be found in Figure 3.1.

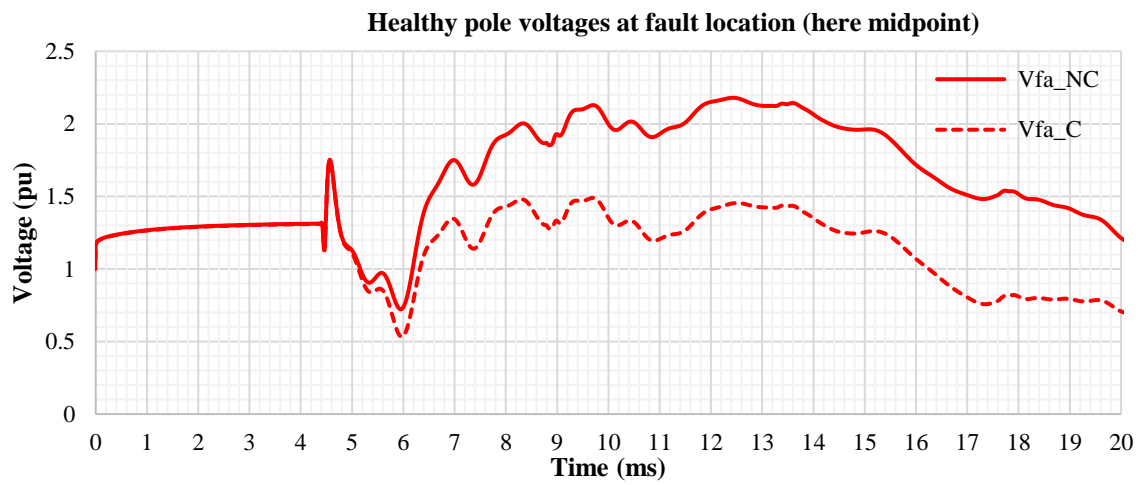
From Figure 4.2, it can be seen that for a fault at the midpoint, the first peak at fault location is at approximately at 4.4 ms and due to positive sequence wave and is the same irrespective of controls. After a short delay of 0.5 ms, the controller starts to change its firing angle and the effect of controls can be observed at the midpoint as voltage deviates from that for the case without controls. The voltages without controls have increased to 2.3 pu, whereas with controls, the voltages remain below 1.7 pu at the midpoint. The voltages at the terminal have also seen the deviation with respect to controls.

In Figure 4.3, for an off-centre fault, it can be observed that the maximum peak is observed at nearly 6.5 ms when the positive waves reach the fault location after reflecting from the farthest terminal. For an off-centre fault, the peak voltage at the fault location is decreased due to the control action.

The results showed discrepancies in voltages with the influence of controls. This shows, that unlike the case with ground return, the effect of controls must be included for determining accurate peak overvoltages. The reason for this is that as only one end of the metallic return conductor is grounded, and so there are additional reflections on the metallic conductor.

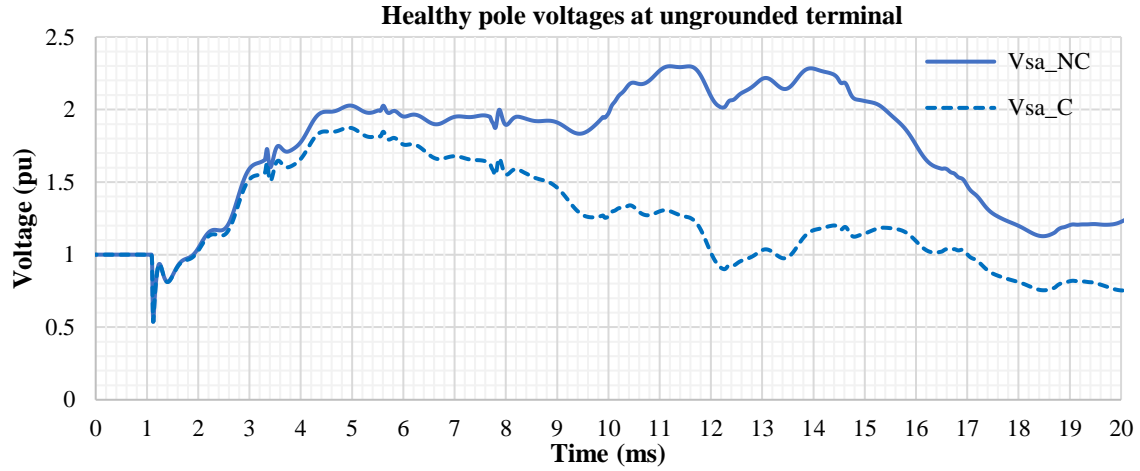


(a)

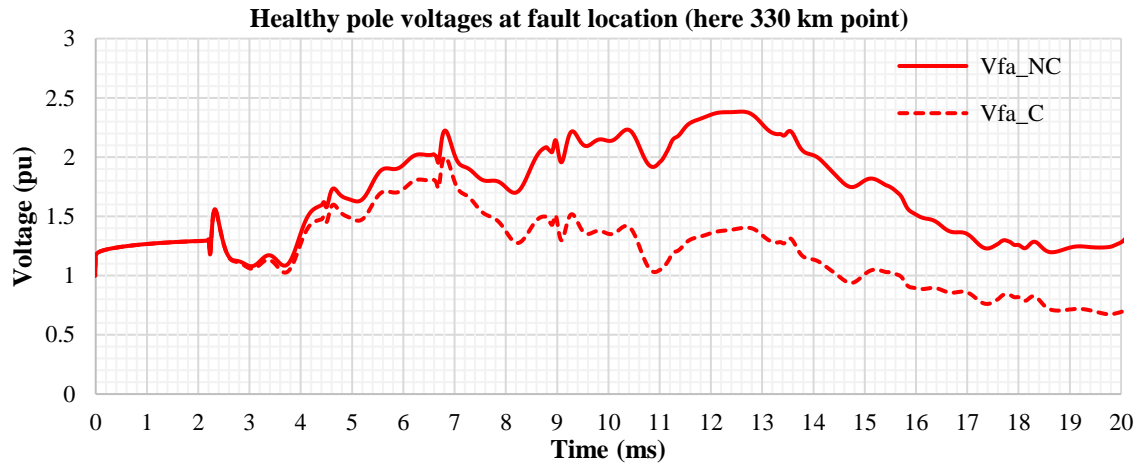


(b)

Figure 4.2 Comparison of healthy pole voltages at (a) ungrounded terminal (b) fault point for a fault at the midpoint of line with controls (C) and without controls (NC)



(a)



(b)

Figure 4.3 Comparison of healthy pole voltages at (a) ungrounded terminal (b) fault point for a fault at 330 km from the ungrounded end, with controls (C) and without controls (NC)

4.4 Faults at different locations along the line

Using the HVdc system used in Section 4.2; ground faults are applied on the negative pole at five equidistant locations: 0 km, 330 km, 660 km, 990 km, 1320 km, from the ungrounded terminal as shown in Figure 4.4 which is drawn for a fault at the midpoint location. As the system is completely symmetric, the overvoltage magnitudes would not change whether the fault was applied on the positive or negative poles.

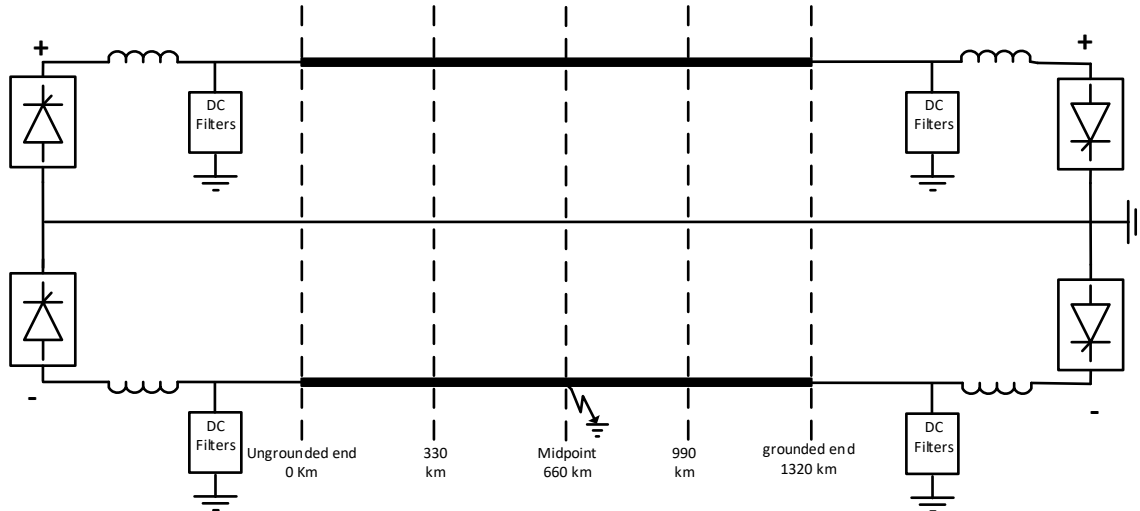


Figure 4.4 dc line with DMR showing five equidistant locations along the line

Typical voltage versus time plots at the converter terminal and fault location for a fault at the midpoint and a fault at the 330 km point are shown in Figure 4.5 and Figure 4.6, respectively.

In Figure 4.5, for a fault at the midpoint, the peak overvoltages at midpoint had reached up to 1.75 pu on the healthy pole and 0.5 pu on DMR when the travelling waves have reached to midpoint after the first reflection at the terminal. However, the highest voltages on the entire line for a midpoint fault are observed at the ungrounded terminal with 1.8 pu on the healthy pole and 1.2 pu on DMR when travelling waves reach the terminal for the second time, i.e., at nearly 6.5 ms.

Similarly, Figure 4.6 shows that for an off-centre fault at 330 km, the maximum overvoltages are observed when travelling waves reflected from the farthest terminal reach the fault point. The peak overvoltages for fault at $1/4^{\text{th}}$ distance from ungrounded terminal reached up to 2 pu on healthy pole and 1 pu on DMR.

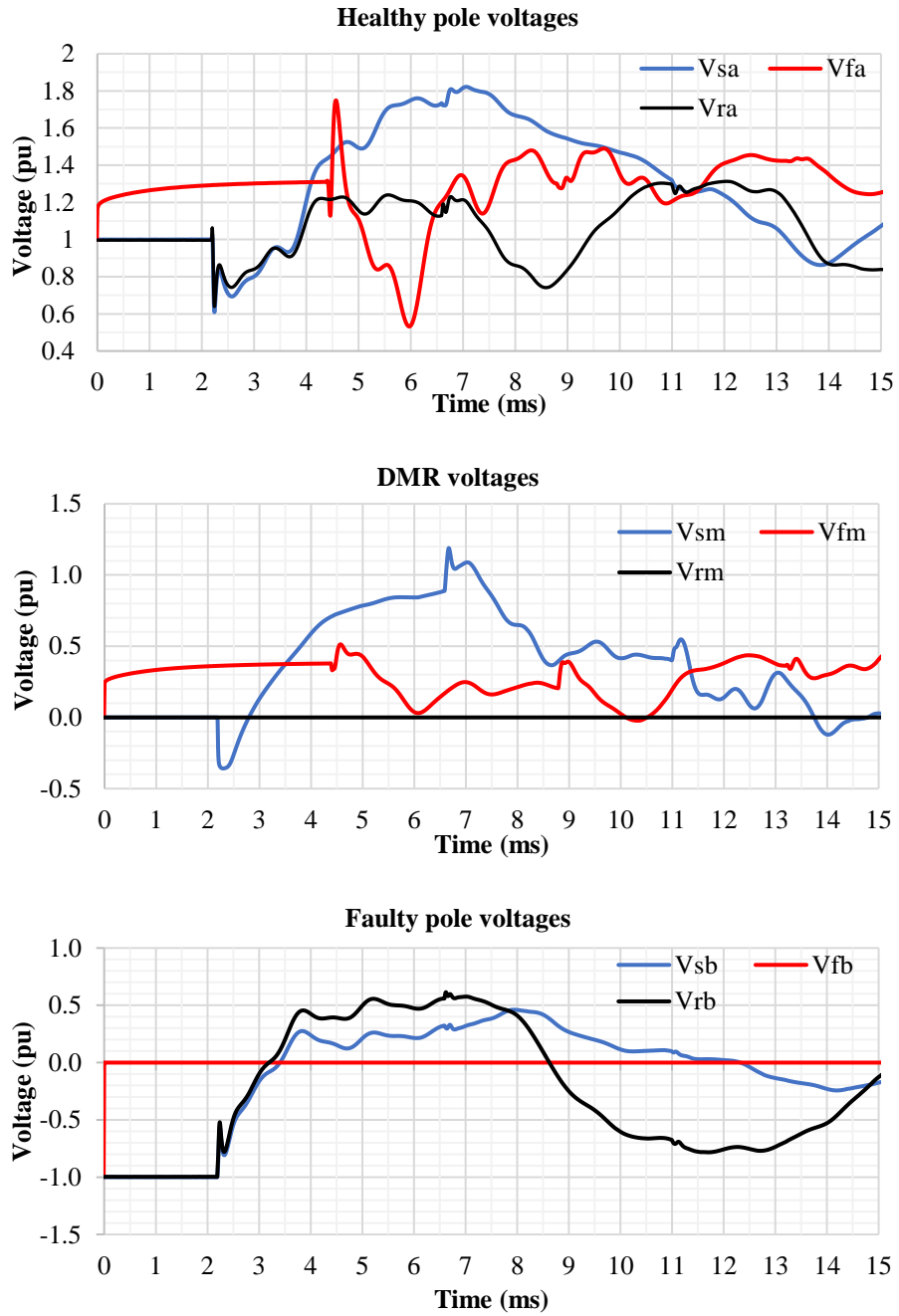


Figure 4.5 Voltage vs time graphs for a fault at the midpoint

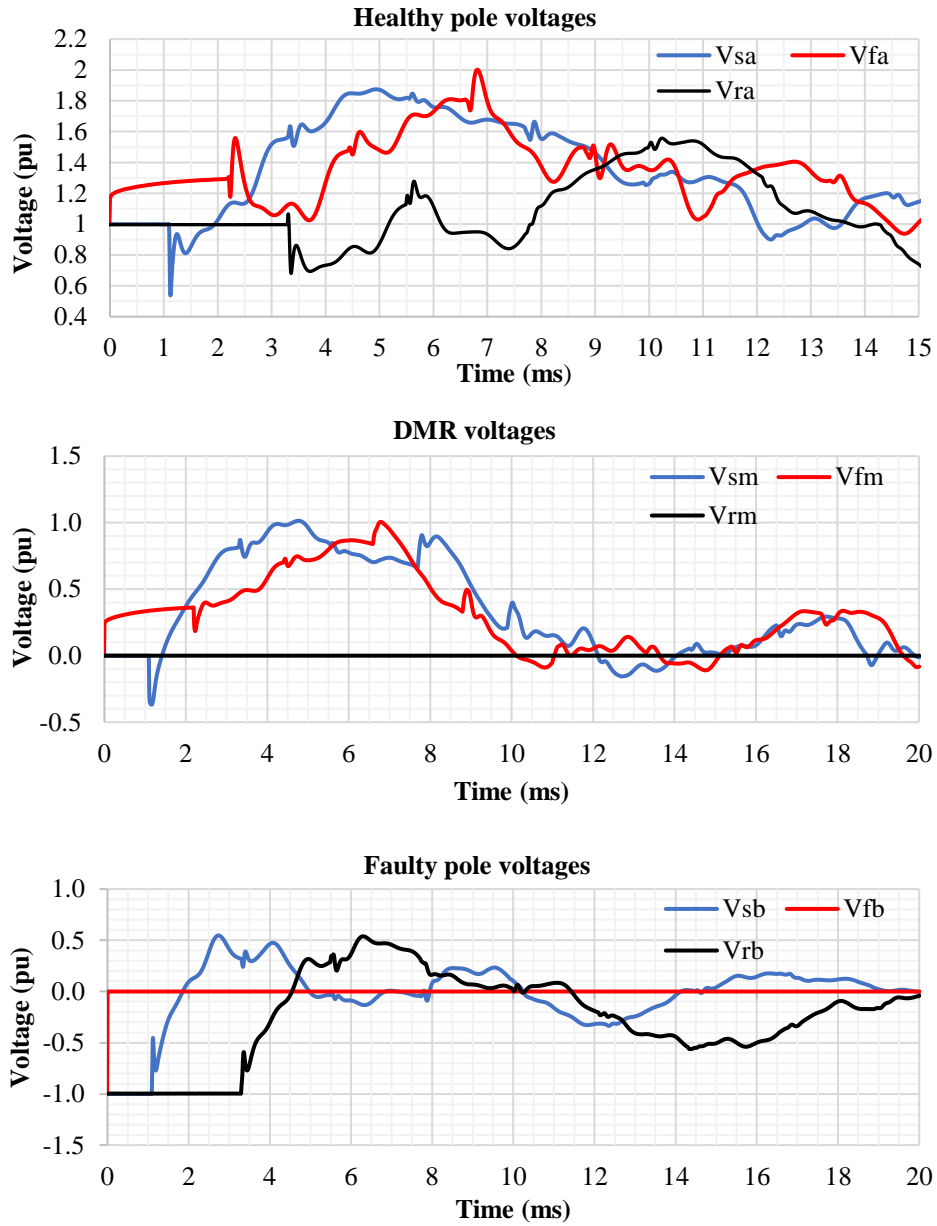


Figure 4.6 Voltage vs time graphs for a fault at 330 km from the ungrounded terminal

Drawing similar graphs for faults at the other locations permits one to develop the maximum overvoltage graphs at various locations along the line for faults at various locations along the line as shown in Figure 4.7.

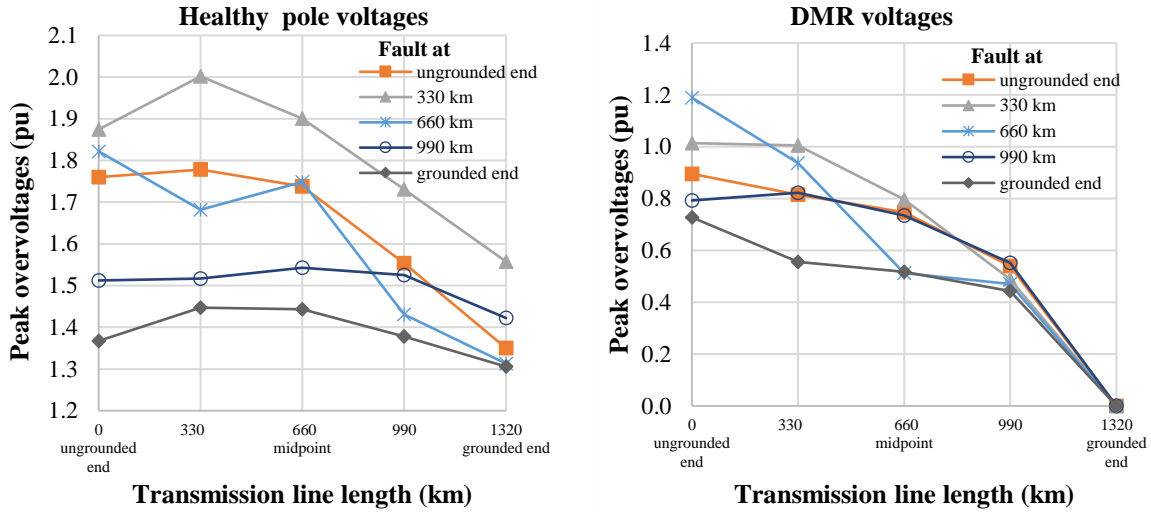


Figure 4.7 Overvoltages on a line with DMR with faults applied at various locations along the length of the line (1320 km).

The following observations can be made from Figure 4.7.

- Regardless of fault location on the negative pole, the first half of the transmission line close to the ungrounded terminal experiences higher voltages than the other half.
- The maximum overvoltage of 2 pu is observed on the healthy pole at 330 km for a fault at the same location.
- DMR conductor experiences the maximum overvoltage of 1.2 pu at the ungrounded end for a fault at the midpoint.

4.4.1 Difference between a dc line with DMR and a dc line with ground return

For the case with ground return as discussed in Section 3.6, the highest overvoltage was observed at the midpoint of the line for a midpoint fault on a pole conductor as shown in Figure 3.8. However, for the case with DMR, they are observed closer to the ungrounded end irrespective of fault location. Also, the most onerous fault location is no longer at the midpoint, but at approximately 1/4th line length (i.e., at 330 km) from the ungrounded end. This is because the converter's neutral point is floating at the ungrounded end, which shifts the neutral voltage to rise during a fault, increasing the healthy pole voltages. Since the maximum overvoltages are not caused by a midpoint fault (unlike the case with ground return), to evaluate the highest overvoltages on a line with DMR, faults have to be applied at different locations along the line as

was done in this section. It is also observed that the maximum overvoltage is slightly larger with the DMR conductor (close to 2 pu) as compared with that for the ground return case (1.8 pu).

A detailed explanation discussing the effects of neutral grounding will be given in Section 4.7. Since the overvoltages up to 2 pu are induced on pole conductors which is higher than the case with ground return, the pole conductor may need to be insulated higher than the dc line with a ground return. The method of reducing overvoltages by use of a surge capacitor at ungrounded neutral is discussed in Section 4.6.

During a fault, the overvoltages are also induced into DMR along with the pole conductor. Since the DMR conductor is not insulated to the same level as the pole conductor, the DMR might flashover earlier than the pole conductor during the monopolar fault. If this occurs, the dc link cannot operate in monopolar mode until the fault on DMR is cleared, compromising the fundamental purpose of having a bipole, redundancy. So, it is important while designing the insulation coordination, that DMR should not flashover during a monopolar fault. It is observed that the overvoltages on DMR had reached up to 1.2 pu on the ungrounded terminal for a fault at the midpoint. However, the overvoltages on DMR have kept decreasing significantly as we go towards the grounded terminal.

4.5 Influence of line length on overvoltages

The above results were for a 1320 km long line. In order to investigate whether the same general conclusions would apply to lines of other lengths, a further study was conducted with the line length reduced to 660 km with the same tower configuration as in Section 4.4. Faults were applied along the line on the negative pole and the voltages on healthy pole and DMR conductor are plotted in Figure 4.8.

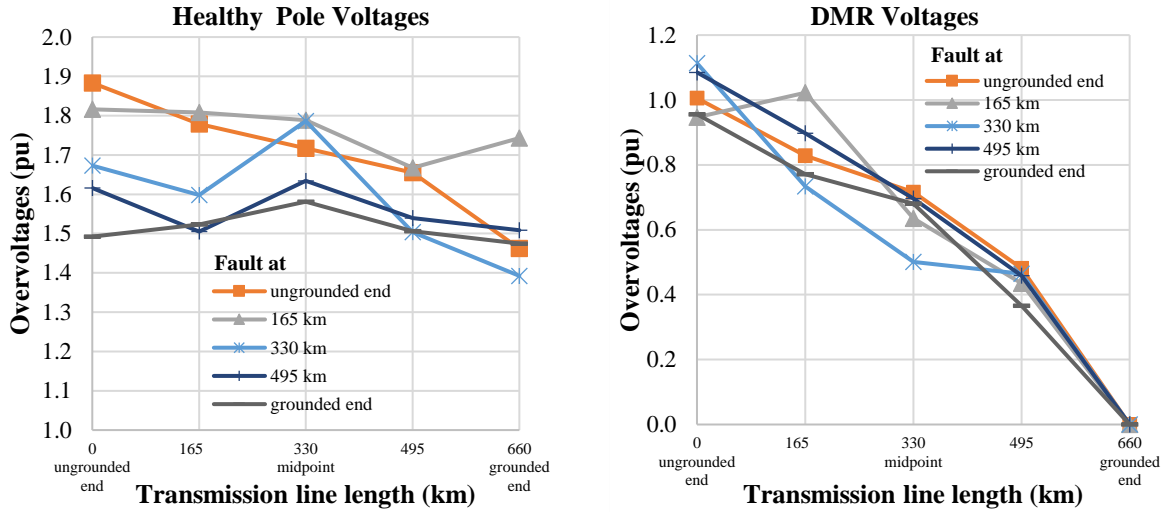


Figure 4.8 Overvoltages on a line with DMR with faults applied at various locations along the length of the line (660 km)

The results show that even with the different line length, the maximum pole overvoltage still occurs closer to the ungrounded end and does not occur for a midpoint fault as was the case with ground return. Also, the maximum overvoltages on the healthy pole and DMR conductor are 1.9 pu and 1.1 pu respectively and are only marginally lower than in the case with the 1320 km line which had an overvoltage of 2.0 pu and 1.2 respectively on the pole and DMR conductors.

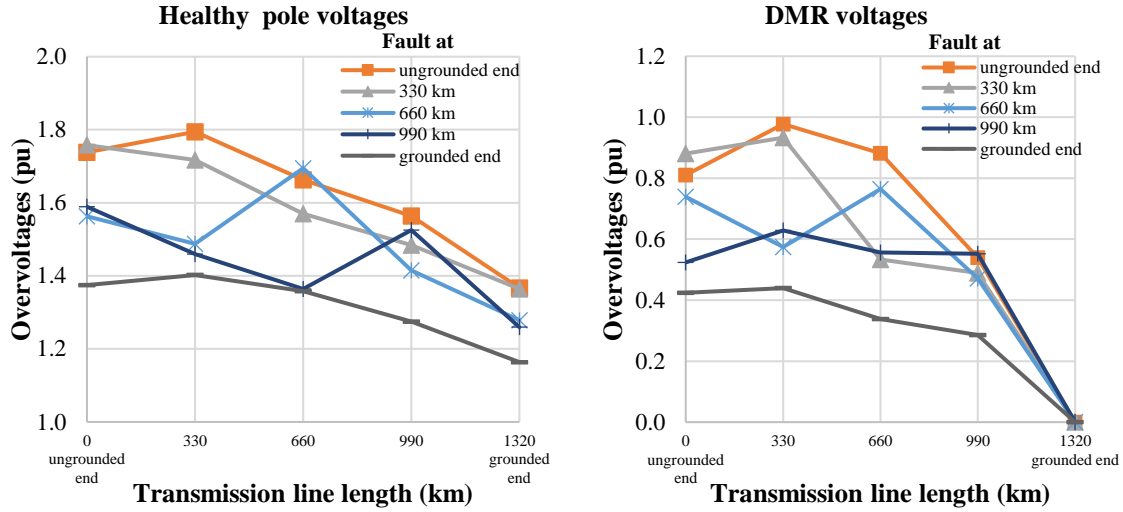
However, the fault location that causes maximum overvoltage on the pole conductor is not at the 1/4th distance point, but at the ungrounded end. Thus, overvoltages depend on the length of the line as well as fault location, requiring detailed investigation for the given line length.

4.6 Effect of neutral surge capacitor

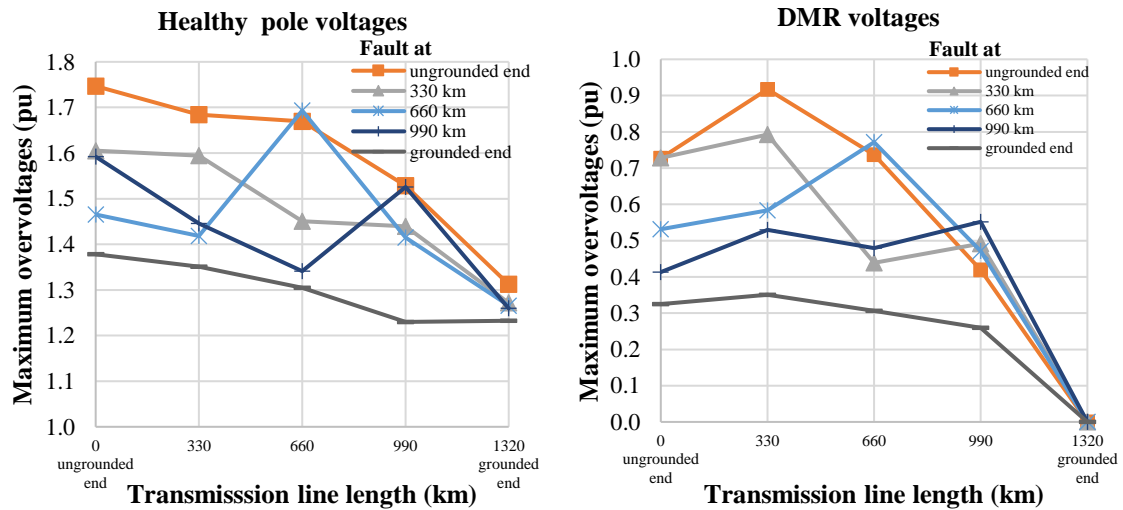
Often a surge capacitor is installed on the ungrounded neutral to reduce the overvoltages by diverting the high frequency surge to the ground. Besides limiting the overvoltages, the surge capacitor at the ungrounded neutral also marginally reduces harmonics entering the dc line by providing a low impedance in-station return path for triplen order harmonic currents [42].

The surge capacitance required for reducing the overvoltage can be determined from the following study.

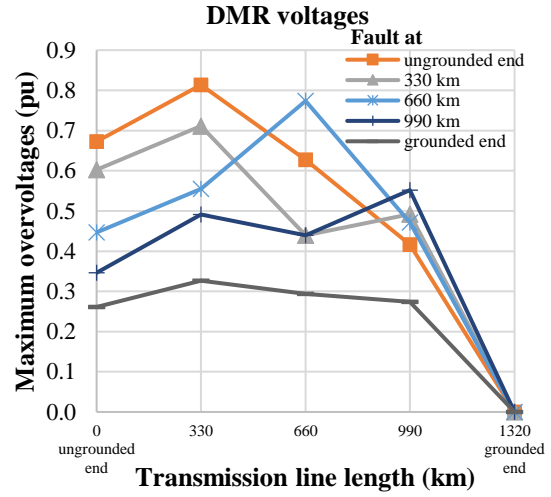
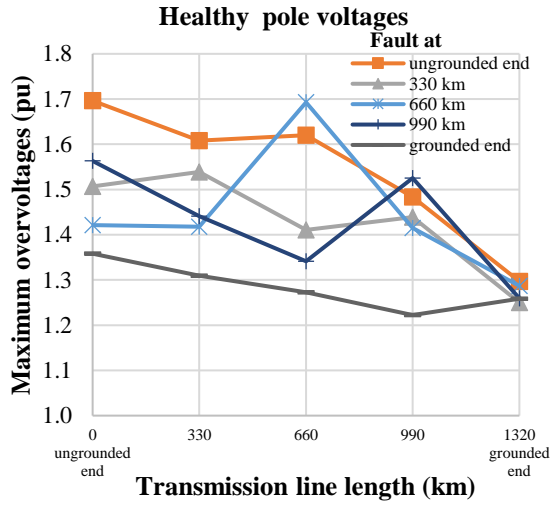
Different surge capacitor of values 10 μF , 20 μF , 30 μF , 40 μF , 50 μF , 100 μF are connected on the ungrounded neutral for the same HVdc system as in Section 4.4 to observe the influence of surge capacitance. Results are plotted in Figure 4.9.



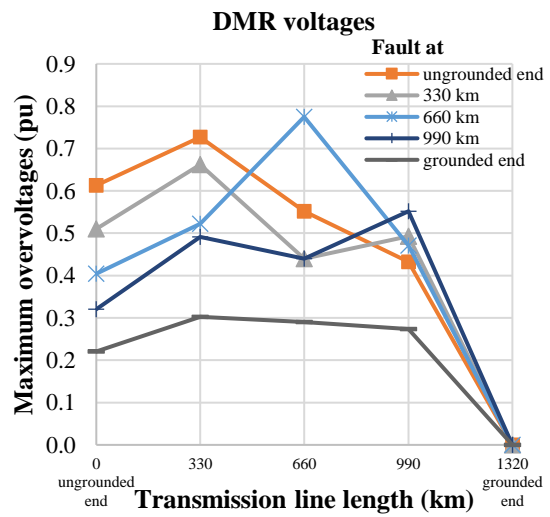
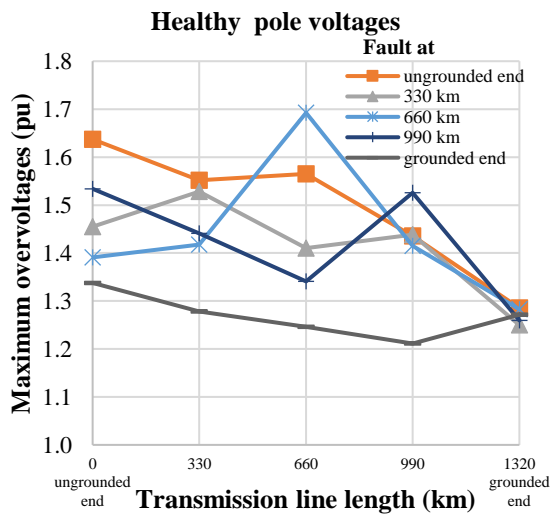
(a) 10 μF



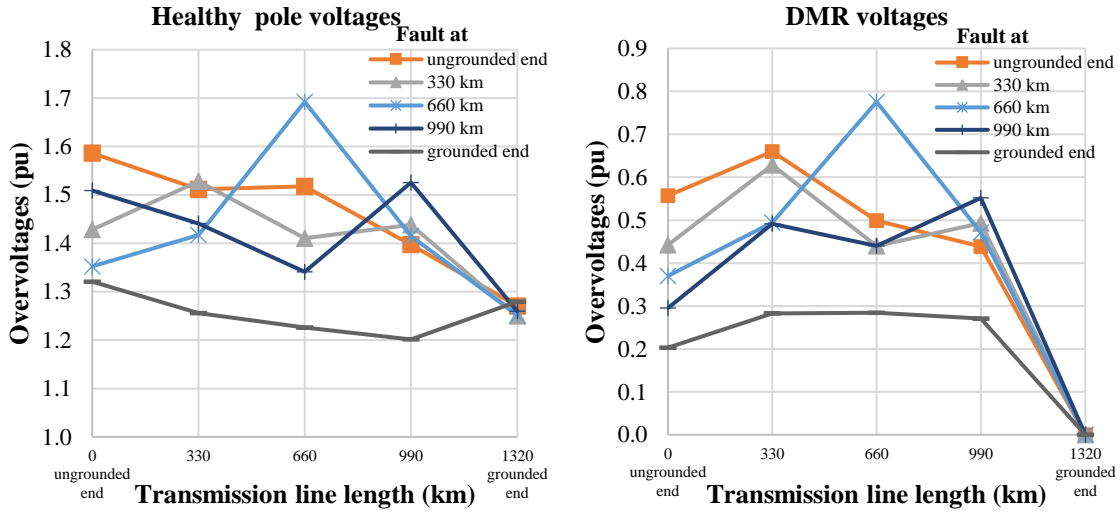
(b) 20 μF



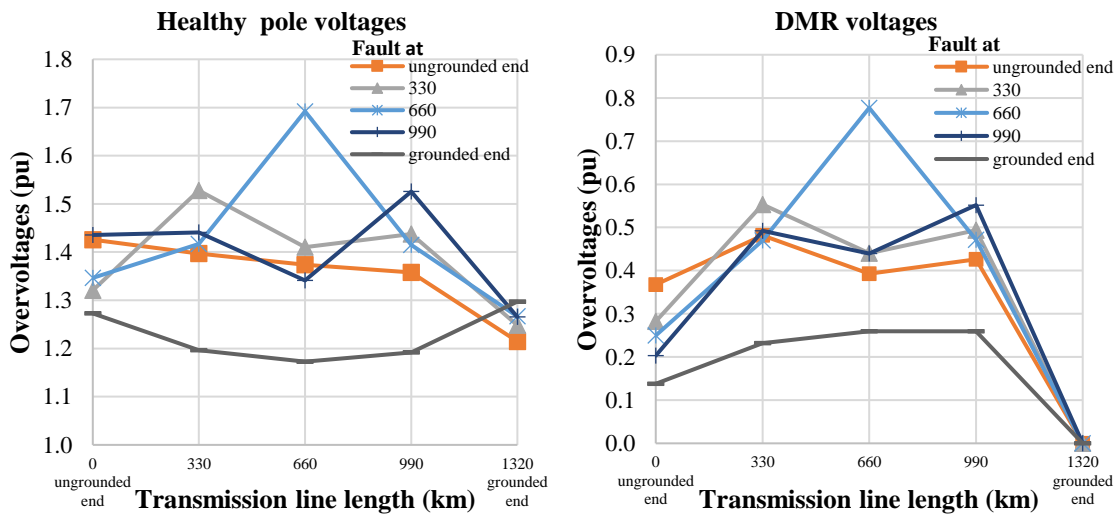
(c) 30 μ F



(d) 40 μ F



(e) 50 μF



(f) 100 μF

Figure 4.9 Comparison of overvoltages along the line with different values of surge capacitor at ungrounded neutral (a) 10 μF (b) 20 μF (c) 30 μF (d) 40 μF (e) 50 μF (f) 100 μF

The results and discussions from Figure 4.9 are summarised below showing the effect of a neutral surge capacitor.

- (a) The maximum overvoltages on the DMR and the healthy pole at the ungrounded terminal are reduced with increasing the value of surge capacitance. However, there is no significant decrease in overvoltages for surge capacitance larger than 30 μF . This can also be observed in Figure 4.10 which shows the variation of peak overvoltages with change in surge

capacitance. In Figure 4.10, faults were applied at various locations and the worst overvoltage on the line (highest overvoltage among all locations) was recorded.

- (b) The maximum overvoltages have been reduced to less than 1.8 pu and 1 pu on healthy pole and DMR respectively by adding a surge capacitance of 10 μF on ungrounded neutral. The maximum overvoltage on the pole conductor with a 10 μF capacitor on ungrounded neutral is now the same as in the case with a ground return.
- (c) For the system studied, the maximum overvoltages on pole and DMR could not be reduced below 1.7 pu and 0.8 pu respectively with the use of a surge capacitor.
- (d) There is no significant effect of surge capacitor on overvoltages at the midpoint for a fault at the same location.
- (e) It is to be noted that surge arresters may also be used in conjunction with surge capacitor to reduce the overvoltages.
- (f) The above analysis shows that a capacitor in the range of 10 μF to 30 μF is a suitable value for the surge capacitor.

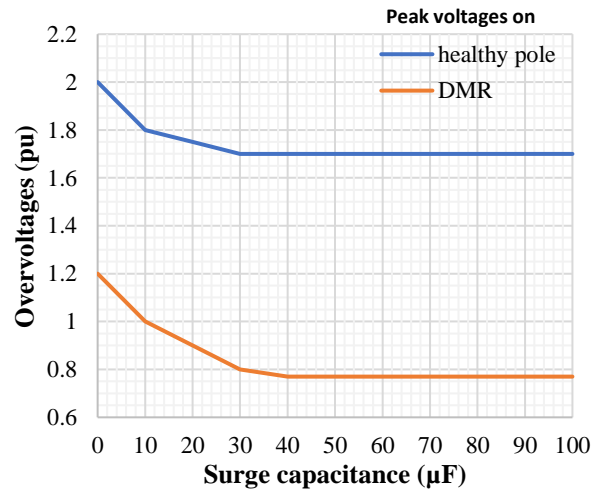


Figure 4.10 Impact of surge capacitance value on maximum overvoltage anywhere on the line for faults at any possible locations

4.7 Theoretical background

4.7.1 Comparison of overvoltages with different neutral grounding and return current path

In this section, an attempt is made to rationalize the influence of DMR on overvoltages using the lattice diagram approach used earlier for dc lines without DMR in Section 3.3. To understand the overvoltage phenomena with DMR, a step by step analysis is conducted in the following sequence:

Case 1: Bipolar HVdc line with both neutrals grounded i.e., with ground return, without DMR (traditional case, as was discussed in Chapter 3).

Case 2: Bipolar HVdc line with only one neutral grounded and without DMR.

Case 3: Bipolar HVdc line with both neutrals grounded but with DMR. Note that this would not be done in practice, because the earth's lower resistance would divert most of the current through the ground rather than through the DMR.

Case 4: Bipolar HVdc line with only one neutral grounded and with DMR. (As was discussed in Section 4.4).

Note that intermediate cases 2 and 3 are not practical but are shown for the purpose of analyzing the differences in voltage waveforms with change in neutral grounding and return current path.

The above cases are summarised in Table 4.1.

Table 4.1 Cases studied for theoretical analysis

	Presence of DMR	Whether converter neutral grounded at	
		Sending end	Receiving end
Case-1	No	Yes	Yes
Case-2	No	No	Yes
Case-3	Yes	Yes	Yes
Case-4	Yes	No	Yes

A lossless transmission line of 1320 km is represented as a Bergeron model at 200 Hz with line parameters shown in Table 4.2. The converters are represented as constant dc sources with a 0.5 H reactor on each pole. Typically, a 2-conductor HVdc line will exhibit two modes (or sequences), i.e., positive and zero sequences, say. Note that with a DMR present and grounded only at one end, there will be 3 modes, say, positive, negative and zero sequences, but the positive and negative sequence modes have the same travel time, assuming that the dc conductors arrangements are symmetric in every way. Hence whether there is a DMR or no DMR, there will be only two distinct travel times as shown in Table 4.2.

A ground fault with zero fault resistance is applied on the negative pole at the midpoint of the line for all four cases. The voltages at the line terminals and the fault point (here midpoint of the line) on the healthy pole and DMR are labelled as shown in Figure 4.11. The voltages on the healthy pole, at neutrals and DMR, are plotted in Figure 4.12 and Figure 4.13 for all four cases.

Table 4.2 Line parameters used for theoretical analysis

Line parameters (at 200 Hz)	Positive (or negative) sequence	Zero sequence
Impedance (Z), in Ω	250	500
Travel time for the full length of line (T) in ms	4.48	5.74

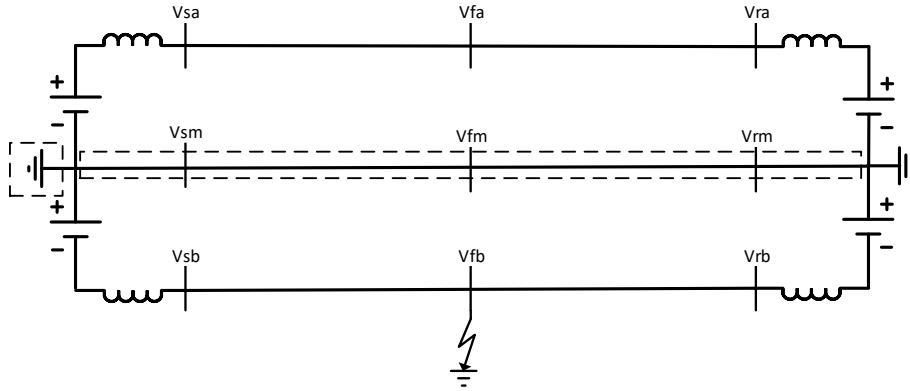


Figure 4.11 Bipolar dc transmission system with fault at the midpoint

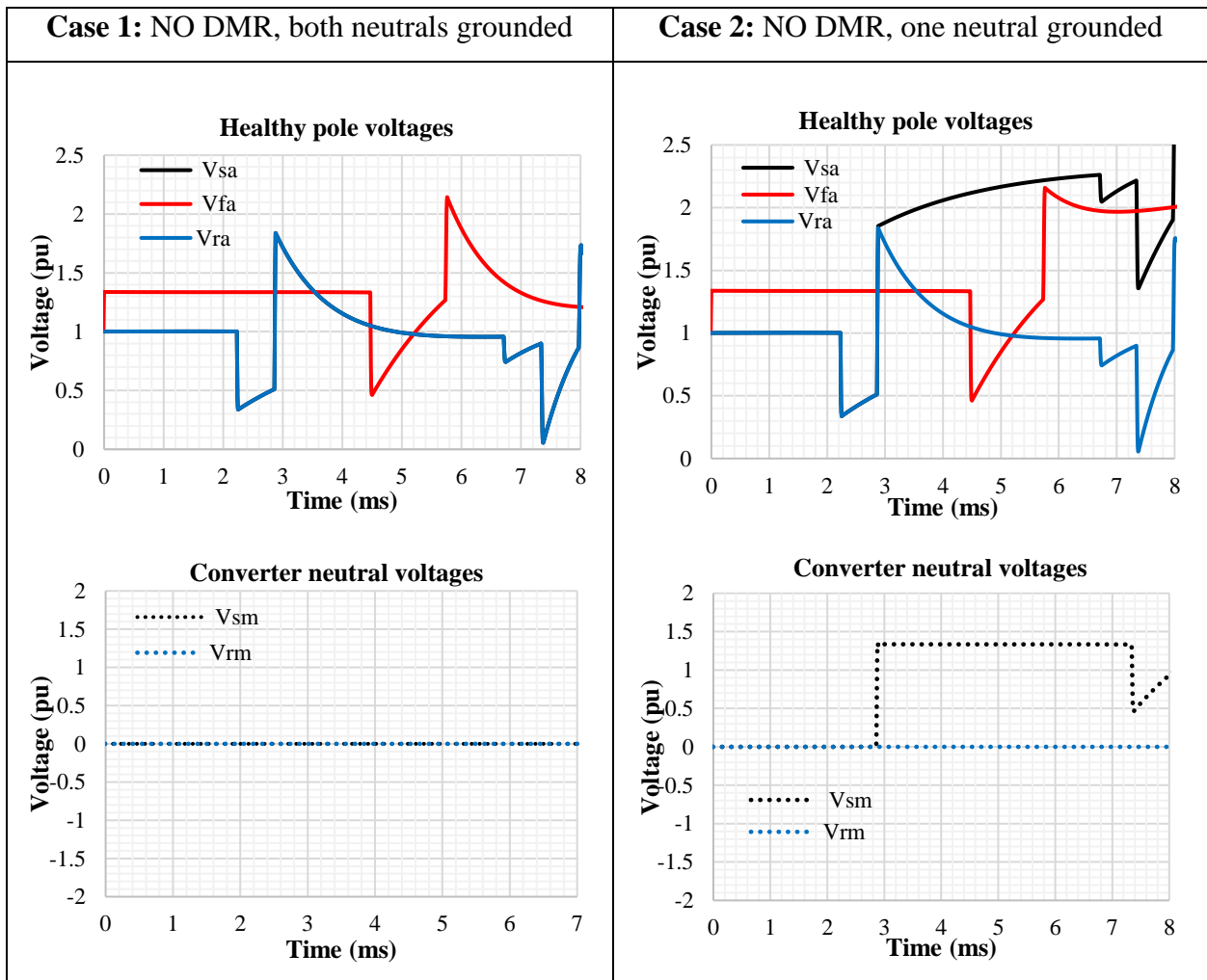


Figure 4.12 Simulated PSCAD voltages for cases 1 and 2 i.e., without DMR

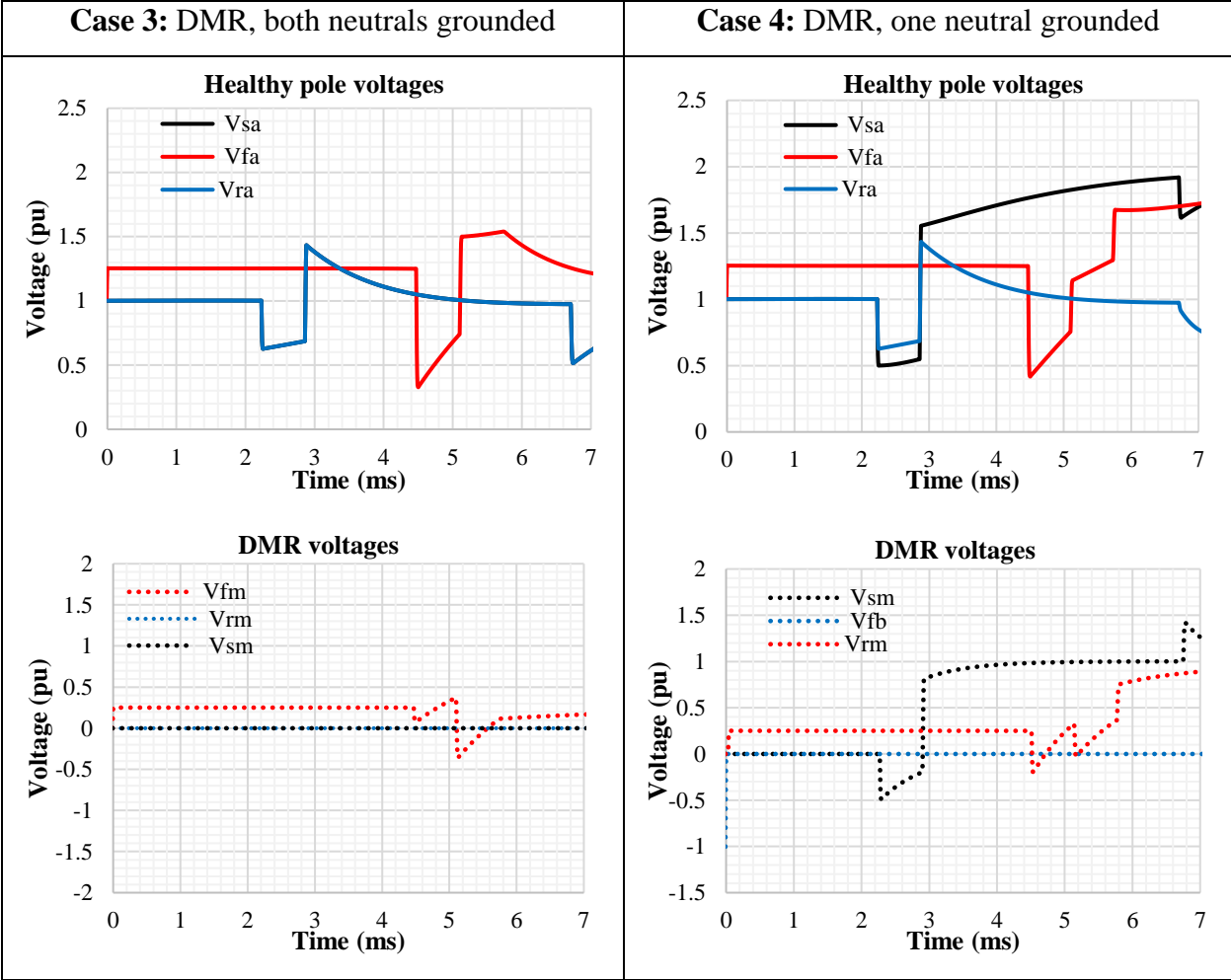


Figure 4.13 Simulated PSCAD voltages for cases 3 and 4 i.e., with DMR

Figure 4.14 shows the voltage waveforms where one neutral is grounded and DMR is present which is essentially the same as the plots for case 4 except plots are given for a longer time period. The waveform shows several jumps, and the reason for these will be given in Section 4.7.2 using Bewley’s diagrams.

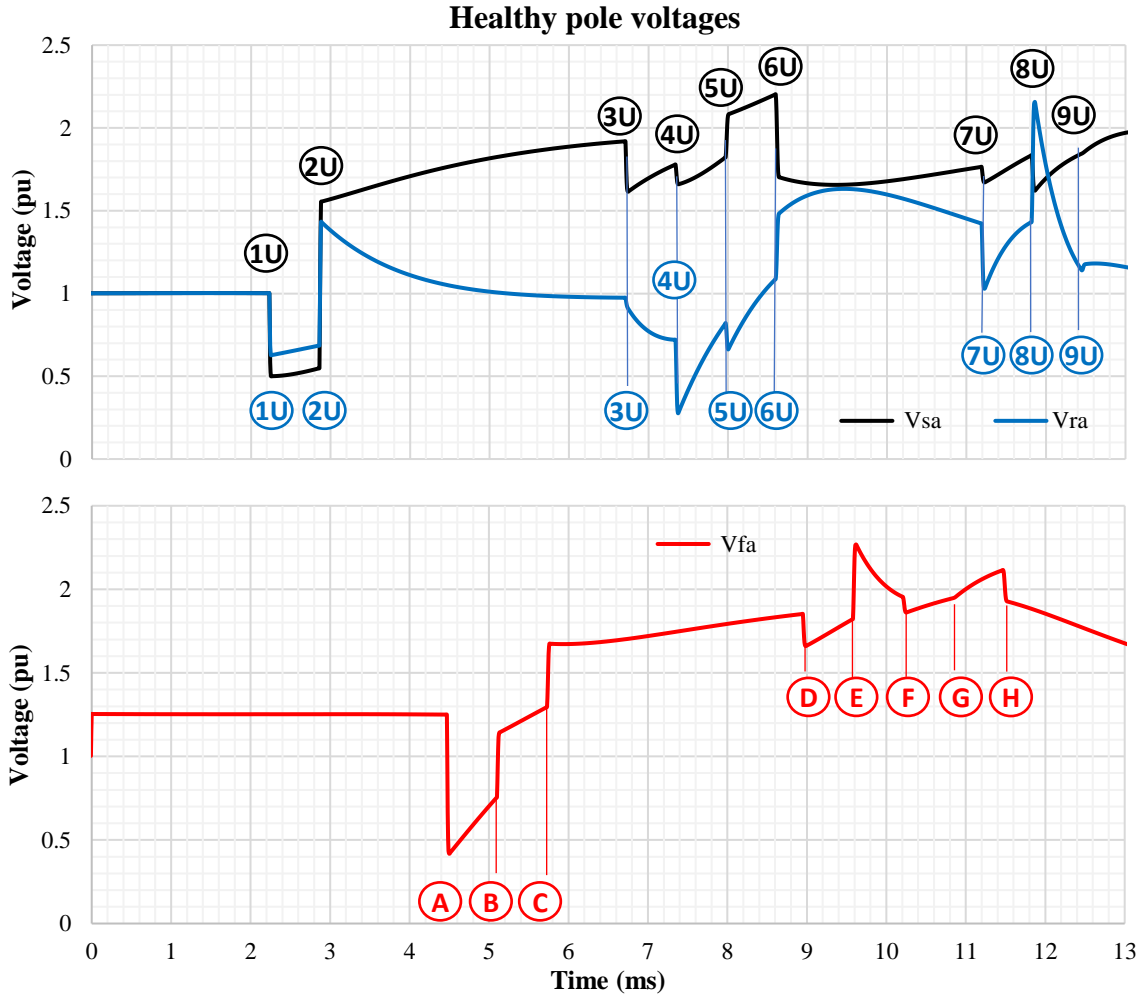


Figure 4.14 Healthy pole voltages on a line with DMR for a fault at midpoint, Case 4

We will now analyze the waveforms in Figure 4.12 and Figure 4.13 show the jumps as seen therein. It should be noted that the travel time for entire length of line for the positive and zero sequence modes are 4.48 ms and 5.74 ms as shown in Table 4.2. Note that for the midpoint fault, the wavefronts will arrive at the line ends in half that time, i.e., the positive sequence front will arrive at approximately 2.2 ms and the zero sequence at approximately 2.9 ms.

- Where the neutrals are grounded at both ends, as in Cases 1 and 3, the terminal voltages are the same at both ends as the line is symmetrical for a midpoint fault whether the DMR is present (Case 3) or absent (Case 1).

- Without DMR and neutral grounded at one end only (Case 2), the healthy pole voltage at the grounded terminal decreases after the zero sequence waves reach the terminal at approximately 2.9 ms, whereas the ungrounded terminal healthy pole voltage kept increasing. This is because the ungrounded neutral voltage is no longer zero and creates an offset in the terminal pole voltage, thereby increasing its magnitude.
- For the cases with DMR present (i.e., Case 3, with both neutrals grounded and Case 4, only one neutral grounded as is modern practice) the instantaneous change in healthy pole voltages at the midpoint immediately after the fault, is lower than the corresponding value in cases without DMR (Cases 1 and 2). Similarly, the change in terminal pole voltages due to positive and zero sequence waves at 2.2 ms and 2.9 ms respectively are lower than the Cases 1 and 2. Hence, the presence of DMR is seen to reduce the instantaneous voltages induced on the healthy pole immediately after the fault.
- In Case 4 (DMR, one neutral grounded), the change in ungrounded terminal pole voltages at 2.2 ms and 2.9 ms are higher than the respective voltage changes at the grounded terminal.
- An additional reflection can be observed on midpoint voltages at 5.1 ms for cases with DMR (Cases 3 and 4) which is not observed in previous cases with a ground return. This extra voltage jump is due to unsymmetrical reflections of travelling waves at both terminals and can be understood with help of a lattice diagram for the cases with DMR discussed in the next section.

4.7.2 Lattice diagram for the case with DMR (i.e., Case 4)

The lattice diagram for the case where the ground return is used with both neutrals grounded is shown in Section 3.3. In this section, the lattice diagram for the case with DMR as shown in Figure 4.15, is discussed. For the case with DMR, because of the three conductors on the line, there are three modes, positive, negative and zero sequence on the transmission line. The positive and negative sequence modes have exactly equal travel times. In the lattice diagram, the vertical axis shows the times of wavefront arrival for the positive and zero sequence waves. The solid line indicates a positive sequence, and the dotted line is zero sequence waves. The horizontal axis represents the distance between both terminals.

Similar to Section 3.3, every time instant where waves meet at the midpoint, ungrounded terminal and grounded terminal is named as A, B, C....; 1U,2U,3U.... and 1G,2G,3G.... respectively and are identified on the healthy pole voltages as a function of time and in lattice diagram are shown in Figure 4.14 and Figure 4.15 respectively.

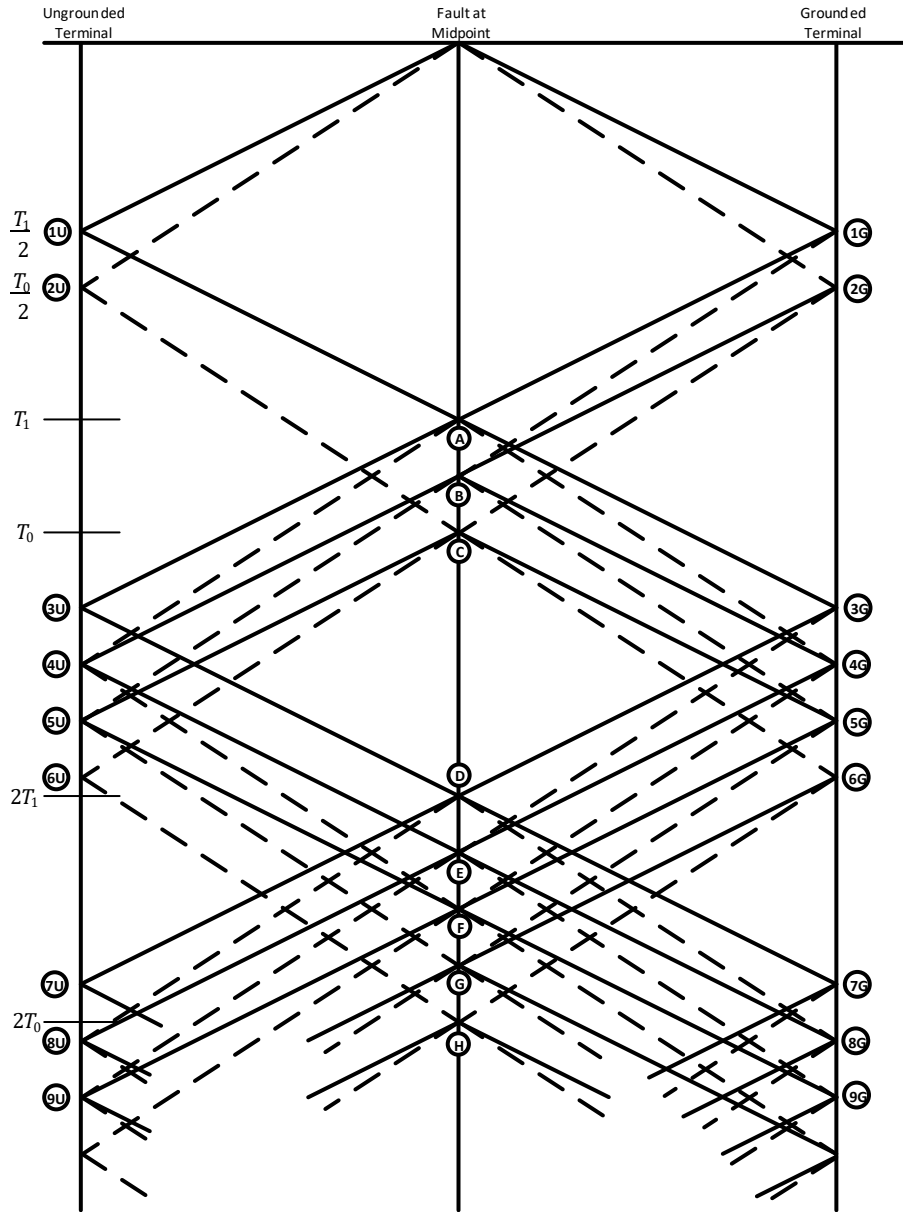


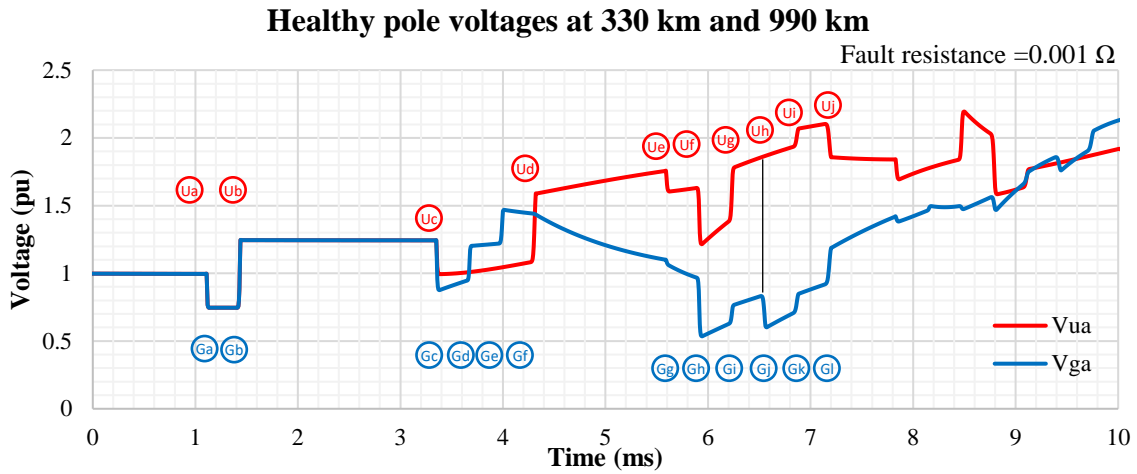
Figure 4.15 Lattice diagram for the case with DMR for a fault at the midpoint

The following observations and conclusions can be drawn from Figure 4.14 and Figure 4.15 for a fault at the midpoint,

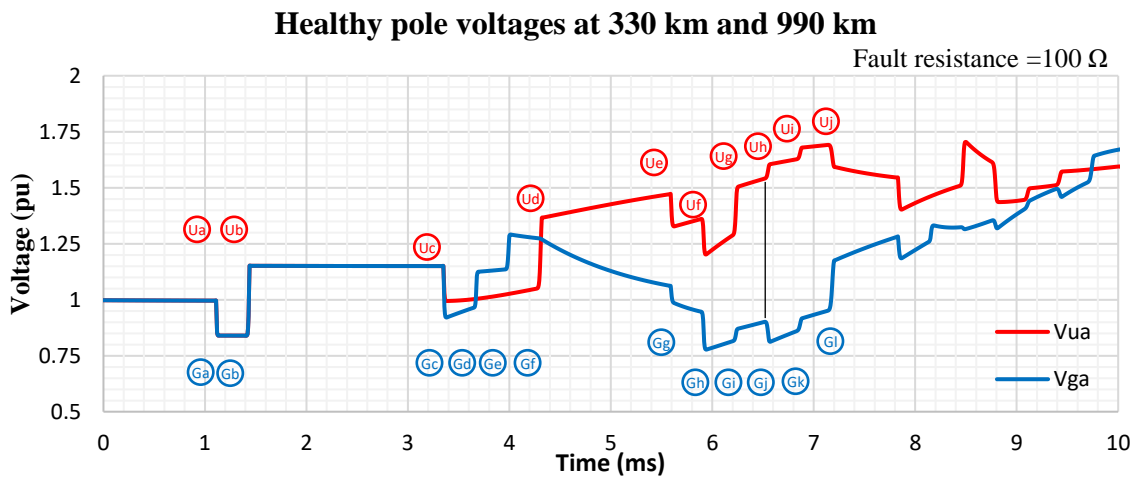
- For a dc transmission system without DMR with grounded neutrals (case 1), a positive sequence wave arriving at a terminal, is reflected as another positive sequence wave, and the same is the case with the zero sequence wave, i.e., each wave reflects in the same mode (as shown in Figure 3.5). However, for the case with DMR (Case 4), the two halves of the line are no longer symmetric, as only one neutral is grounded. The reflections at the ungrounded terminal (at points 1U, 2U, 3U... in Figure 4.15) are the same as in the previous case i.e., with ground return, see Figure 3.5; but at the grounded terminal, each positive and zero sequence wave reflect as both positive and zero sequence waves (e.g., points 1G, 2G, 3G on the lattice diagram in Figure 4.15).
- As a result of these unsymmetric reflections, the positive and zero sequence waves from the grounded terminal arrive concurrently and cause the observed jump at point B in the simulation plot of Figure 4.14. These additional voltage jumps on the dc line with DMR are discussed in Section 4.7.3.

4.7.3 Voltage waveforms at other locations (330 km and 990 km) using lattice diagrams

Figure 4.16 shows the PSCAD simulated voltage waveforms at 330 km and 990 km locations for the fault case as previous, i.e., midpoint fault on the negative pole. The voltage at 330 km and 990 km are labelled as V_{ua} and V_{ga} respectively. In Figure 4.16 (a) the fault resistance is 0Ω , and in Figure 4.16 (b) it is 100Ω . To examine the voltages at 330 km and 990 km on the lattice diagram, two dotted lines are drawn parallel to vertical axis which represents the voltages at these two locations as shown in Figure 4.17.



(a)



(b)

Figure 4.16 Healthy pole voltages at 330 km and 990 km for a fault at the midpoint of the line with fault resistance of (a) 0.001Ω (b) 100Ω

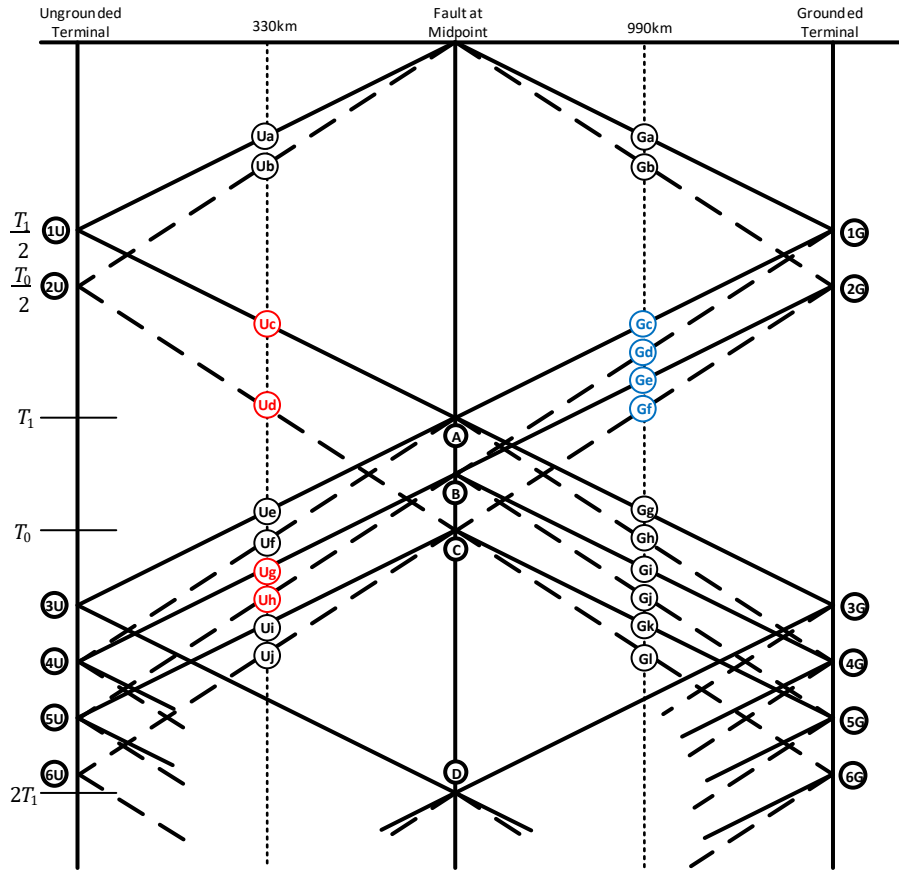


Figure 4.17 Lattice diagram showing the voltages at two locations at 330 km and 990 km

The following observations and conclusions can be drawn from Figure 4.16 and Figure 4.17,

- When travelling waves reach towards midpoint after their first reflection at the ungrounded terminal, we can observe only two voltage jumps U_c , U_d at the 330 km location while at the same time at the 990 km location, four voltage jumps are observed namely G_c , G_d , G_e , G_f . These voltage jumps can be noticed in Figure 4.16 (a) (b) and agrees with the lattice diagram. This demonstrates that the travelling wave reflections are not symmetrical for a ground fault on an HVdc line with DMR grounded at one end.
- The voltage jumps, U_g and U_h at the 330 km location are due to the transmitted waves coming from the grounded end towards the ungrounded end from point B and cannot be observed in Figure 4.17 (a). However, when the fault resistance is increased to 100Ω , voltage jump U_h can be identified as shown in Figure 4.16 (b). It is also worth noting that the overall overvoltage has decreased on the line with an increase in the fault resistance.

4.8 Chapter summary

In this chapter, the phenomena of overvoltages on a dc line with DMR are studied. The influence of grid control on overvoltages is identified and that accurate determination of peak overvoltages requires the controls to be considered. Simulations are conducted to find the overvoltages on a line with DMR for faults at different locations along the line. The effect of neutral surge capacitor at the ungrounded terminal is studied for various values capacitance. Results showed that voltages up to 2 pu and 1.2 pu are observed on healthy pole and DMR respectively. However, these voltages can be reduced to 1.8 pu and 0.8 pu by adding a 30 μ F capacitor at ungrounded neutral.

An explanation of overvoltages for the case with DMR is given using a lattice diagram and the differences between the case with ground return and DMR are discussed.

5 Conclusions and future work

This thesis investigated the overvoltages caused due to a pole-ground fault, on a dc overhead transmission line with a dedicated metallic return. Concluding remarks and recommendations for future studies in this work are also presented in this chapter.

5.1 Conclusions

The phenomenon of ground fault overvoltages on a dc overhead transmission line with DMR is different from the line with a ground return since only one converter neutral is grounded and the other is floating in the former while both neutrals are grounded for the latter. This affects how the reflections of travelling waves happen at the terminals and alter the magnitude of overvoltages. The overvoltages on systems with metallic return were studied using EMT simulations and lattice diagram techniques. The important observations and conclusions are summarized below.

5.1.1 Observations and conclusions

- a. The maximum overvoltages on the line with ground return occur due to the first reflections of travelling waves at the terminal and midpoint. This is not true for the case with the DMR.
- b. The influence of controls must be taken into consideration while calculation of overvoltages with DMR for more realistic results. We always find that with controls, the overvoltages are considerably lower than when they are not considered. Therefore, considering controls will result in an economic line because of lower overvoltages.
- c. On the dc line with DMR, the highest overvoltage on the healthy pole is caused for faults occurring in the section between the ungrounded end and the midpoint. Whereas highest overvoltage on the DMR conductor is due to fault at the midpoint of the line similar to the ground return case.
- d. Also, the maximum pole overvoltage magnitude is somewhat larger than with ground return, e.g., 2.0 pu as opposed to 1.8 pu in the simulation results for the 1320 km line. The rationale for the increase in the overvoltages on the line with DMR is because one neutral of the bipole is left ungrounded, which shifts the healthy pole voltage to increase at the ungrounded terminal.
- e. The overvoltages on the DMR conductor is significantly large for a conductor which is grounded at one end. For the 1320 km line, maximum overvoltage of 1.2 pu is observed.

- f. Placing a surge capacitance at ungrounded neutral can significantly reduce the DMR overvoltage and marginally reduce the pole overvoltage as well. For the 1320 km long line example, adding a 30 μF surge capacitor at the ungrounded neutral reduces the worst case overvoltage on the DMR from 1.2 pu to 0.8 pu; and on the pole conductor from 2.0 pu to 1.7 pu.
- g. There is a diminishing return with the size of the surge capacitance at ungrounded neutral. For example, in the studied example, the reduction in overvoltage was negligible once the surge capacitance exceeded 40 μF .
- h. The magnitude of maximum overvoltages were different with different line lengths, indicating the necessity to calculate overvoltages for each length of line.
- i. Lattice diagrams were used to gain a qualitative understanding of overvoltage phenomena. The reflections of travelling waves and their constructive and destructive interferences can explain the timing and severity of the overvoltages in the two cases.

5.1.2 Recommendations arising from the research

The following general recommendations are applicable based on the study cases for the assumed transmission line and tower structures. Although some parametric analysis was conducted (e.g., change in line length), the analysis should be repeated by the interested parties for their specific configurations.

- a. The pole conductors of the HVdc line with DMR should be insulated higher than the traditional dc line with a ground return if no surge capacitors are used.
- b. DMR conductor insulation should be designed to withstand a minimum of 0.8 pu overvoltage if only surge capacitors are present on the ungrounded neutral. If DMR is not insulated to the required insulation level, DMR might also flashover during the monopolar fault along with the pole conductor, resulting in an entire bipole shut down for a pole on one conductor which fundamentally defies the purpose of having a bipole instead of a monopole.

5.2 Suggestions for future studies

- a. An in-depth analytical analysis of travelling wave reflections at terminals can be studied similar to Kimbark by developing mathematical equations for the fault on dc line with DMR [33].
- b. The effect of surge arresters in conjunction with surge capacitors can be studied to further reduce the overvoltages on the dc line.
- c. A similar method of study investigating the overvoltages could also be performed on an overhead line with Voltage Source Converter technology.

REFERENCES

- [1] J. Arrillaga, *High voltage direct current transmission*, 2nd ed. vol. 2. London: The Institution of Electrical Engineers, 1998.
- [2] N. G. Hingorani, “High-voltage dc transmission: A power electronics workhorse,” *IEEE Spectr.*, vol. 33, no. 4, pp. 63–72, 1996.
- [3] M. H. Nguyen and T. K. Saha, “Power loss evaluations for long distance transmission lines,” *Aust. Geotherm. Energy Conf.*, no. 1, pp. 307–312, 2009.
- [4] M. Milligan, E. Ela, E., J. Hein, T. Schneider, G. Brinkman, and P. Denholm, “Renewable electricity futures study: Bulk electric power systems-operations and transmissions planning,” *Natl. Renew. Energy Lab.*, vol. 4, 2012.
- [5] O. E. Oni, I. E. Davidson, and K. N. I. Mbangula, “A review of LCC-HVdc and VSC-HVdc technologies and applications,” *EEEIC 2016 - Int. Conf. Environ. Electr. Eng.*, 2016.
- [6] A. Alassi, S. Bañales, O. Ellabban, G. Adam, and C. MacIver, “HVdc transmission: technology review, market trends and future outlook,” *Renew. Sustain. Energy Rev.* 112, pp. 530–554, 2019.
- [7] Hitachi ABB, “HVdc classic reference list,” Sep. 2017. [Online]. Available: <https://search.abb.com/library/Download.aspx?DocumentID=POW0013&LanguageCode=en&DocumentPartId=&Action=Launch>. [Accessed Jan. 31, 2021].
- [8] R. Nayak, R. Sasmal, S. Sen, B. Pelly, and P. Riedel, “Experience with blocking devices during monopolar operation of ± 500 kV, 2000 MW Talcher-Kolar HVdc system in India,” *41st Int. Conf. Large High Volt. Electr. Syst. 2006, CIGRE Session*, vol. 41, pp. B4–204, 2006.
- [9] The China Electric Power Research Institute, *UHV transmission technology*. London: Academic Press, 2017.
- [10] P. Tyagi, Bagadia. V, Kumar. R, Anand. A, Goswami. M. M, and Jha. I. S, “Design challenges for ± 800 kV, 3000 MW HVdc Champa-Kurukshetra transmission link with dedicated metallic return (DMR) - User’s perspective,” CIGRE B4-109, 2014.

- [11] M. M. G. Ebin Cherian, V.Singh, M.S. Rao, and B.B. Mukherjee, “Feasibility study for 6000 MW Raigarh (Chattisgarh) - Pugalur (Tamil Nadu) -Trichur (Kerala) HVdc transmission,” *CIGRE SC B4 Int. Colloq. HVdc STATCOM, Agra, 2015*.
- [12] Noosuk. A, Mermork. T, Semjan. A, Rahman. M. S, Dawood. A. R, Ismail. S. B, Kurth. R. D, and Atmuri. S. R. “Commissioning experience of the 300 MW Thailand - Malaysia interconnection project,” *Proc. IEEE Power Eng. Soc. Transm. Distrib. Conf.*, vol. 2, pp. 1004–1009, 2002.
- [13] M. Sampei, H. Magoroka, and M. Hatano, “Operating experience of Hokkaido-Honshu high voltage direct current link,” *Proc. of 1996 Transm. and Distrib. Conf. and Expo.*, vol. 12, no. 3, pp. 158–163, 1996, doi: 10.1109/TDC.1996.545929.
- [14] M. Takasaki, T. Sato, S. Hara, and H. Chishaki, “Operating experiences and results of on-line extinction angle control in Kii Channel HVdc link.” *CIGRE B4-212,2014*
- [15] IEEE Standards Association, *National Electrical Safety Code C2-2007 Edition*. 2006.
- [16] R. E. Harrison, “Insulation Requirements for dc Transmission Lines,” *Electra*, pp. 21–32, 1975.
- [17] J. A. Jardini, J. F. Nolasco, J. F. Grahan, and G. Bruske, *Impacts of HVdc lines in the economics of HVdc projects (CIGRE Brochure 388)*, CIGRE Jt. Work. Gr. B2/B4/C1, no. 17, pp. 1-162, 2009.
- [18] D. J. Melvold, P. C. Odam, and J. J. Vithayathil, “Transient Overvoltages on HVdc Bipolar Line during Monopolar Line Faults,” *IEEE Trans. Power Appar. Syst.*, vol. 96, no. 2, pp. 591–601, 1977, doi: 10.1109/T-PAS.1977.32370.
- [19] N. G. Hingorani, “Monopolar metallic return operation of long distance HVdc transmission systems,” *IEEE Trans. Power Appar. Syst.*, vol. PAS-93, no. 2, pp. 554–563, 1974, doi: 10.1109/TPAS.1974.294003.
- [20] S. Sasaki and H. Matsubara, “Fault surges on HVdc transmission lines in both bipolar operation and monopolar metallic return operation modes and comparison with field results,” *IEEE Power Eng. Rev.*, vol. AS-101, no. 7, pp. 2221-2228, July 1982., doi: 10.1109/MPER.1982.5521105.

- [21] V. Jankov and M. Stobart, "HVdc System Performance with a Neutral Conductor," *2010 Int. Conf. High Volt. Eng. Appl. ICHVE 2010*, pp. 188–191, 2010, doi: 10.1109/ICHVE.2010.5640834.
- [22] R. A. Walling, M. Sublich, D. J. Lorden, and S. A. Doe, "Simultaneous Pole and Neutral Faults on an HVdc Line with a Dedicated Metallic Return," *IEEE Trans. Power Deliv.*, vol. 5, no. 2, pp. 1129–1136, 1990, doi: 10.1109/61.53131.
- [23] R. B. Sinha, "UHVdc transmission with dedicated metallic return," *Proc. IEEE Int. Conf. Technol. Adv. Power Energy, TAP Energy 2015*, pp. 485–488, 2015, doi: 10.1109/TAPENERGY.2015.7229667.
- [24] E. W. Kimbark, (1971). *Direct current transmission (Vol. 1)*. Wiley, 1971.
- [25] M. Meisingset and A. M. Golé, "Control of capacitor commutated converters in long cable HVdc-transmission," *Proc. IEEE Power Eng. Soc. Trans. Dist. Conf. (Cat No. 01CH37194)*, vol. 2, pp. 962–967, 2001, doi: 10.1109/pesw.2001.917003.
- [26] R. A. Keswani, "Identification of fault in HVdc converters using wavelet based multi-resolution analysis," *first int. conf. on emerging trends in engineering and technology*, pp. 954–959, July 2008., doi: 10.1109/ICETET.2008.150.
- [27] E. Uhlmann, *Power transmission by direct current*. New York: Springer Science & Business Media, 2012.
- [28] M. D. Heffernan, J. Arrillaga, C. P. Arnold, and K. S. Turner, "Recovery From Temporary HVdc line faults," *IEEE Power Engineering Review*, vol. PER-1, no. 4, pp. 58-58, April 1981, doi: 10.1109/MPER.1981.5511410.
- [29] CIGRE WG 14.21-TF1, "Summary of Existing Ground Electrode Designs," *Cigre*, 1998.
- [30] CIGRE WG B4.61, "General Guidelines for HVdc Electrode Design", TB-675, *Cigre*, 2017.
- [31] N. Knudsen and F. Iliceto, "Contribution to the electrical design of EHVdc overhead lines," *IEEE Trans. Power Appar. Syst.*, vol. PAS-93, no. 1, pp. 233–239, 1974, doi: 10.1109/TPAS.1974.293937.
- [32] S. Hara, M. Hirose, M. Hatano, S. Kinoshita, H. Ito, and K. Ibuki, "Fault protection of

- metallic return circuit of KII channel HVdc system,” *IEE Conf. Publ.*, no. 485, pp. 132–137, 2002, doi: 10.1049/cp:20010531.
- [33] E. W. Kimbark, “Transient overvoltages caused by monopolar ground fault on bipolar dc line: Theory and simulation,” *IEEE Trans. Power Appar. Syst.*, vol. PAS-89, no. 4, pp. 584–592, 1970.
- [34] N. G. Hingorani, “Transient overvoltage on a bipolar HVdc overhead line caused by dc line faults,” *IEEE Trans. Power Appar. Syst.*, vol. PAS-89, no. 4, pp. 592–610, 1970.
- [35] R. F. Stevens, “Design of the Celilo - Sylmar 800-kV dc line - BPA section,” *IEEE Trans. Power Appar. Syst.*, vol. PAS-86, no. 7, pp. 916–922, 1967.
- [36] H. W. Dommel, “Digital Computer Solution of Electromagnetic Transients in Single - and Multiphase Networks,” *IEEE Trans. Power Appar. Syst.*, vol. PAS-88, no. 4, pp. 388–399, 1969, doi: 10.1109/TPAS.1969.292459.
- [37] J. R. Marti, “Accurate modelling of frequency-dependent transmission lines in electromagnetic transient simulations,” *IEEE Trans. Power Appar. Syst.*, vol. PAS-101, no. 1, pp. 147–157, 1982, doi: 10.1109/TPAS.1982.317332.
- [38] C. L. Fortescue, “Method of symmetrical co-ordinates applied to the solution of polyphase networks,” *Trans. Am. Inst. Electr. Eng.*, vol. 37, pp. 1027–1140, 1918, doi: 10.1109/T-AIEE.1918.4765570.
- [39] M. Szechtman, “First benchmark model for HVdc control studies.,” *Electra*, no. 135, pp. 55–73, 1991.
- [40] B. Peng, H. Rao, T. Shang, C. Feng, D. Wang, H. Huang, P. Riedel, K. Sadek, “Basic design aspects of Gui-Guang HVdc power transmission system,” *PowerCon 2002 - 2002 Int. Conf. Power Syst. Technol. Proc.*, vol. 1, pp. 533–537, 2002, doi: 10.1109/ICPST.2002.1053599.
- [41] CIGRE AG B4.04, “Compendium of HVdc Schemes Throughout The World,” *Cigre*, 2005.
- [42] N. L. Shore, A. Gangadharan, A. Kumar, and A. K. Skytt, “dc Harmonic Filter Design and Mitigation of Induced Fundamental Frequency Currents for the NEA 800 kV HVdc Multi-terminal Project,” *CIGRE SC B4 Int. Colloq. HVdc STATCOM, Agra*, 2015.